branes were then incubated with HRPO-conjugated antimouse IgG Ab (1:2000). Signals were detected using Super Signal West Femto Maximum Sensitivity Substrate (Pierce, Rockford, IL) and the LAS-3000 image analyzer (Fujifilm, Tokyo, Japan).

### *TNF-α assay*

As described above, cells ($4 \times 10^5$ cells/well) were stimulated by PFA-fixed SV-T2/OX40L or by PFA-fixed SV-T2/control cells ($2 \times 10^5$ cells/well), for the times indicated, in 12-well plates. For the determination of TNF-α production, culture supernatants and cell lysates ($5\text{-}6 \times 10^6$ cells/ml) were collected, and the concentrations of TNF-α were assayed using the Quantikine human TNF-α kit (R&D). The protein concentrations in cell lysates were determined using the advanced protein assay reagent.

### *Detections of apoptosis in primary T cells*

Human peripheral blood mononuclear cells (PBMCs) were isolated from heparinized (5 U/ml) blood of normal healthy donors using standard density gradient centrifugation and a human lymphocyte separation medium (Sigma). The cells at the interface were collected and washed three times in PBS containing 2% FCS. PBMCs were resuspended at $1 \times 10^6$ cells/ml in RPMI medium, supplemented with 20 U/ml rhIL-2. Each well of 12-well plates was coated with 5 μg/ml anti-hCD3 mAb (clone OKT-3) for 1 h at 37°C and washed three times in PBS. Then, 1 ml of the cell suspension was dispensed into individual wells and cultured in the presence of either rhIL-12 or rhIL-4 at 20 ng/ml for 3 days at 37°C in a 5% $CO_2$ humidified incubator. The activated cells were harvested, adjusted to $2 \times 10^5$ cells/ml, and further stimulated using the same conditions at days 3 and 6. Activated PBMCs were harvested on day 9, in 20 U/ml rhIL-2-containing RPMI medium, and were then cocultivated for 24 h with either PFA-fixed SV-T2/OX40L or with PFA-fixed SV-T2/control cells at a cell to cell ratio of 1:1. Anti-hOX40L mAb (5A8) was added at 20 μg/ml to prevent OX40–OX40L interaction. The cells were then stained by Cy5-labeled anti-hCD4 mAb (OKT-4) followed by FITC-labeled annexin V to detect apoptosis. Apoptotic cells in the $CD4^+$ T cell gate were detected by FACSCalibur.

## RESULTS

### *Combined stimulation of ACH-2/OX40 cell line cells with OX40L and TNF decreases HIV-1 production by inducing rapid apoptosis*

We have previously reported that the chronically HIV-1-infected cell line ACH-2/OX40 produces large amounts of HIV-1 within 24 h, following stimulation by either coculture with OX40L-expressing cells or by the addition of TNF-α or -β. Such activation of HIV-1 replication is mediated primarily through activation of the NF-κB pathway.[38] In the present study, we examined the effect of dual stimulation by OX40L and TNF-α (or TNF-β, data not shown) on HIV-1 production. In contrast to the previously documented increase in HIV-1 production by activation via the ligation of either OX40 or TNF-R alone, dual stimulation of these two receptors resulted in a marked reduction of HIV-1 production in ACH-2/OX40 cells (Fig. 1A). The morphology of the ACH-2/OX40 cells was markedly altered following 24 h of dual stimulation (Fig. 1B). This morphological effect was associated with the induction of rapid apoptosis, as determined by apparent cell death (Fig. 1C) and by annexin V-FITC/PI staining (Fig. 1D). Of interest was the finding that all the dual receptor-stimulated ACH-2/OX40 cells became apoptotic as early as 9 h after stimulation, before HIV-1 production was detectable (Fig. 1A and D).

### *Dual receptor-induced activation also affects HIV-1 production in other HIV-1-infected cell line cells*

To determine whether this HIV-1 reduction and this rapid cell death, induced by such dual receptor activation, were unique to the ACH-2/OX40 cells or whether they are general for all types of HIV-1-infected cells expressing these two receptors, a series of other HIV-1 productively or chronically in-

**FIG. 4.** Involvement of the OX40 cytoplasmic tail and of the caspase cascade in the induction of apoptosis of Molt-4/CCR5-OX40 cells. (**A**) Molt-4/CCR5-OX40 (M/R5-OX40), Molt-4/CCR5-OX40del (M/R5-OX40del), and Molt-4/CCR5-control (M/R5-control) cells were cocultured with PFA-fixed SV-T2/OX40L (OX40L) or with PFA-fixed SV-T2/control (Control) cells, at a cell-to-cell ratio of 2:1 in the absence (Medium) or in the presence of 2 ng/ml TNF-α for 24 h. (**B**) The blocking of apoptosis of the M/R5-OX40 cells, induced by OX40L or by OX40L/TNF-α stimulation, by a caspase inhibitor, z-VAD-fmk. The caspase inhibitor z-VAD-fmk (z-VAD) was added, before stimulation, to M/R5-OX40 cells at a final concentration of 100 μM. The pretreated M/R5-OX40 cells were cocultured with PFA-fixed SV-T2/OX40L (OX40L) or with PFA-fixed SV-T2/control (Control) cells, at a cell-to-cell ratio of 2:1 in the absence (Medium) or in the presence of 2 ng/ml TNF-α for 3, 6, and 24 h. Apoptotic and live cells were determined by a standard dual staining method using annexin V-FITC and PI. The cells were classified as undamaged cells, annexin V(−)/PI(−); early apoptotic cells, annexin V(+)/PI(−); and late apoptotic cells and necrotic cells, annexin V(+)/PI(+). The stimulating cells, which included the PFA-fixed SV-T2/OX40L or SV-T2/control cells, were included within the region of annexin V(+)/PI(+) cells (about 20% of the total cell number). The percentage of live cells is shown at the lower left quadrangle of each dot plot. (**C**) The cell lysates obtained from the M/R5-OX40 cells stimulated by PFA-fixed SV-T2/OX40L (OX40L) or by PFA-fixed SV-T2/control (Control) cells, at a cell-to-cell ratio of 2:1 for 6 h, were treated with an equal volume of 2× sample buffer without 2-mercaptoethanol, separated by SDS–PAGE, using a 12.5% gel, and then transferred to Immobilon-P Transfer Membrane. After blocking, the membranes were incubated with the primary anticaspase-8 and anti-caspase-3 mAbs (1:1000) followed by horseradish peroxidase-conjugated antimouse IgG Ab (1:2000). The reaction was detected using Super Signal West Femto Maximum Sensitivity Substrate and an image analyzer. Representative results from three independent experiments are shown.

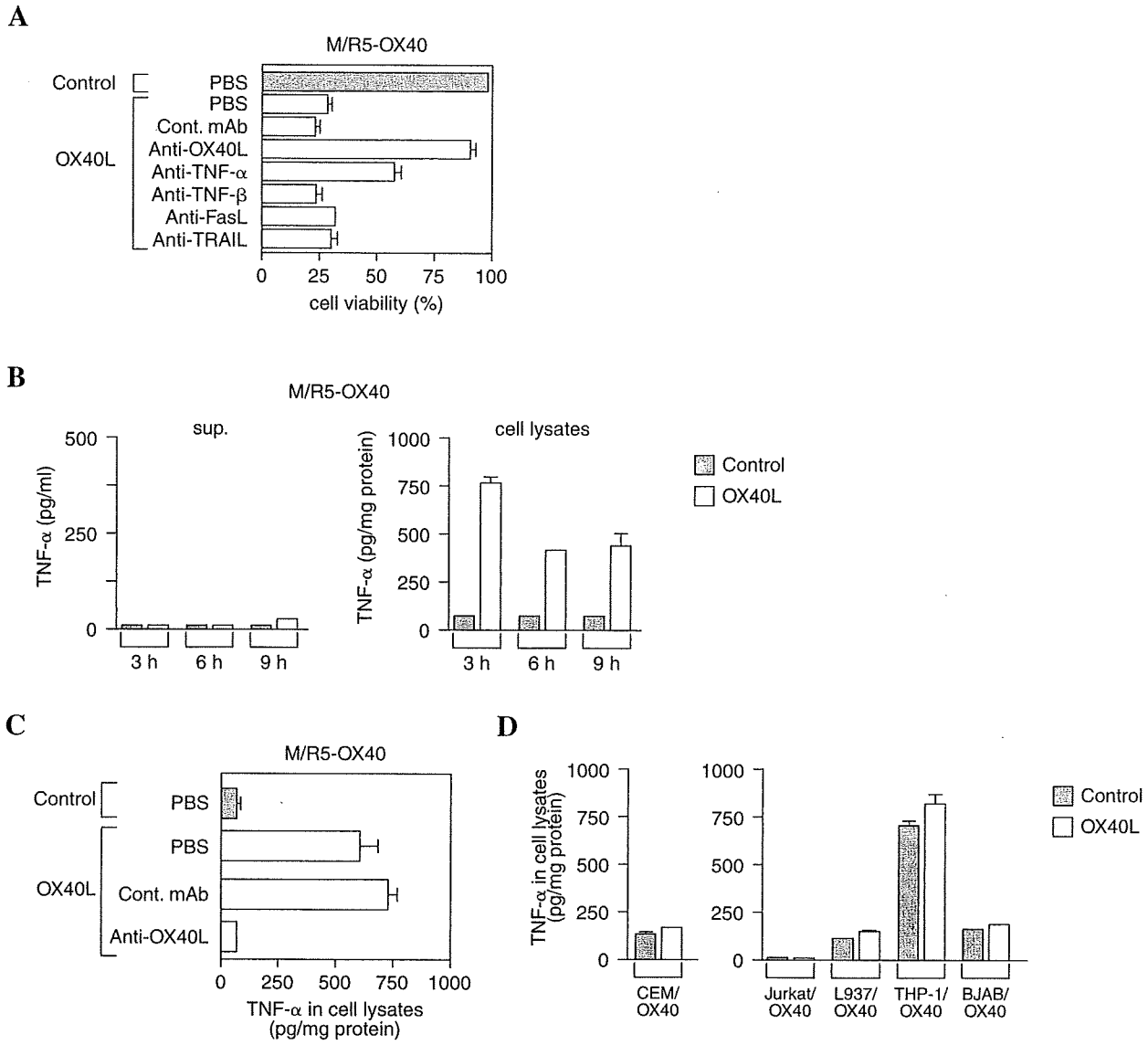


**FIG. 5.** OX40-induced apoptosis in Molt-4/CCR5-OX40 cells is mediated by endogenous TNF-$\alpha$. (**A**) Molt-4/CCR5-OX40 (M/R5-OX40) cells were stimulated by PFA-fixed SV-T2/OX40L (OX40L) or by PFA-fixed SV-T2/control (Conrol) cells in the presence or in the absence of anti-hTNF-$\alpha$ (Anti-TNF-$\alpha$, 30-100 $\mu$g/ml), anti-hTNF-$\beta$ (Anti-TNF-$\beta$, 100 $\mu$g/ml), anti-hTRAIL (Anti-TRAIL, 100 $\mu$g/ml), anti-hFasL (Anti-FasL, 100 $\mu$g/ml), and anti-hOX40L (Anti-OX40L, 10 $\mu$g/ml) neutralizing mAb or with isotype control (Cont. mAb) for 24 h. Live cells were determined by annexin V-FITC/PI staining, followed by FACS analysis. (**B**) M/R5-OX40 cells were stimulated for 3, 6, and 9 h by PFA-fixed SV-T2/OX40L (OX40L) or by PFA-fixed SV-T2/control (Control) cells. TNF-$\alpha$ concentrations were determined in the culture supernatants (sup., left panel) and in the cell lysates (cell lysates, right panel) by an hTNF-$\alpha$ sandwich ELISA. (**C**) M/R5-OX40 cells were stimulated by PFA-fixed SV-T2/OX40L (OX40L) or by PFA-fixed SV-T2/control (Control) cells in the presence or in the absence of anti-hOX40L neutralizing mAb (Anti-OX40L, 10 $\mu$g/ml) or with isotype control (Cont. mAb) for 6 h. TNF-$\alpha$ concentrations were determined in the cell lysates. (**D**) The cells were stimulated by PFA-fixed SV-T2/OX40L (OX40L) or by PFA-fixed SV-T2/control (Control) cells for 6 h, in the case of CEM/OX40 cells, and for 24 h in all other cells. TNF-$\alpha$ concentrations were determined in the culture supernatants and in the cell lysates. The data presented are the mean values ± SD of triplicate determinations. Representative results from three independent experiments are shown.

fected cell lines transfected with OX40 were examined. These cell lines included the OX40-transfected T cell line, Molt-4/IIIB, Molt-4/IIIB-OX40 (M/IIIB-OX40), and the promonocytic cell line, U1, U1/OX40. The M/IIIB-OX40 cells produced relatively large amounts of HIV-1 upon stimulation with either OX40L or with TNF-$\alpha$. The U1/OX40 cells produced significant levels of HIV-1 following stimulation with TNF-$\alpha$, but produced little following ligation using OX40L. On the other hand, dual receptor activation with OX40L and TNF-$\alpha$ dramatically reduced HIV-1 production in M/IIIB-OX40 and in U1/OX40 cells, similar to our findings using ACH-2/OX40 cells (Fig. 2A). In M/IIIB-OX40 cells, moderate cell death was observed following OX40L stimulation, while dual stimulation, with OX40L and TNF-$\alpha$, induced rapid cell death (data not

shown). In U1/OX40 cells, moderate cell death was induced only following dual stimulation (data not shown). The role of OX40/OX40L was underscored by the observation that antibody blockade of OX40L inhibited HIV-1 activation following OX40L stimulation. Antibody blockade also reversed HIV-1 reduction following dual stimulation with OX40L and TNF-$\alpha$ in ACH-2/OX40 and in M/IIIB-OX40 cells (Fig. 2B). Similarly, anti-OX40L blocking mAb partially or completely inhibited the cell deaths induced in ACH-2/OX40 and M/IIIB-OX40 cells following dual stimulation with OX40L and TNF-$\alpha$ (data not shown). The reduction of HIV-1 production resulting from dual receptor activation was also observed in the acutely HIV-1 NL4-3-infected Molt-4/CCR5-OX40 (M/R5-OX40) cells (Fig. 2C). This effect was also reversed by anti-OX40L blocking mAb. However, stimulation with OX40L alone did not enhance HIV-1 activation in acutely infected M/R5-OX40. The viability of the HIV-1 acutely infected M/R5-OX40 cells was rapidly reduced not only following dual stimulation with OX40L and TNF-$\alpha$ but also stimulation with OX40L alone as compared to ACH-2/OX40 and M/IIIB-OX40 cells (data not shown). This effect on cell viability was completely reversed with anti-OX40L blocking mAbs (data not shown). Therefore, these results support the view that OX40 stimulation by its natural ligand, OX40L, combined with stimulation by TNF-$\alpha$, leads to a significant reduction of HIV-1 production, which is associated with rapid cell death, not only in an ACH-2 cell line, but also in Molt-4/IIIB, U1, and HIV-1 acutely infected Molt-4/CCR5 cell lines.

### *OX40 ligation-mediated cell death occurs independently of HIV-1*

To determine whether the cell death of cells overexpressing OX40, induced by the stimulation with OX40L and/or TNF-$\alpha$, was intrinsic to the cytopathic effects of HIV-1 infection, we established a series of HIV-1-negative/OX40-positive and control vector transfectants. These cells were stimulated by coculture with $OX40L^+$ cells in the presence or absence of TNF-$\alpha$, followed by analysis of cell viability. As shown in Fig. 3A, cell death was seen in both the M/R5-OX40 and in the CEM/OX40 cells following stimulation by OX40L, and, furthermore, dual stimulation with OX40L and TNF-$\alpha$ synergistically accelerated the rate of cell death. In these two cell lines, TNF-$\alpha$ alone, at the doses utilized, had no effect on cell viability. On the other hand, in the case of another T cell line, Jurkat/OX40, and the two $CD4^+$ promonocytic cell lines, U937/OX40 and THP-1/OX40, dual receptor stimulation, but not OX40L stimulation alone, strongly induced cell death. However, the rate of cell death was more moderate in these cell lines than the rate observed with M/R5-OX40 and with CEM/OX40 cells. In contrast, the B cell line BJAB/OX40 was resistant to each of the stimulation protocols utilized above. As shown in Fig. 3B, death of OX40-expressing $CD4^+$ T cells, following stimulation with either OX40L or with OX40L and TNF-$\alpha$, was completely inhibited by anti-OX40L blocking mAb. This shows that OX40 triggering by OX40L was necessary for the induction of cell death. Maximum cell death was observed under close cell-to-cell contact between $OX40^+$ responder and $OX40L^+$ stimulator cells and at higher TNF-$\alpha$ concentrations (more than 2 ng/ml) (Fig. 3C). Therefore, in the absence of HIV-1, OX40-mediated signaling is capable, on its own, of inducing cell death, and the dual stimulation with OX40L and TNF-$\alpha$ leads to an accelerated rate of cell death than stimulation with either ligand alone, which differs with respect to the cell line being studied.

### *OX40-mediated apoptosis in M/R5-OX40 cells is induced by signaling via the cytoplasmic tail of OX40 and by the caspase cascade*

To confirm that the cell death, observed above, was dependent on signal transduction via OX40, we established a cell line expressing a deletion mutant of OX40 that lacked the cytoplasmic tail, Molt-4/CCR5-OX40del (M/R5-OX40del). M/R5-

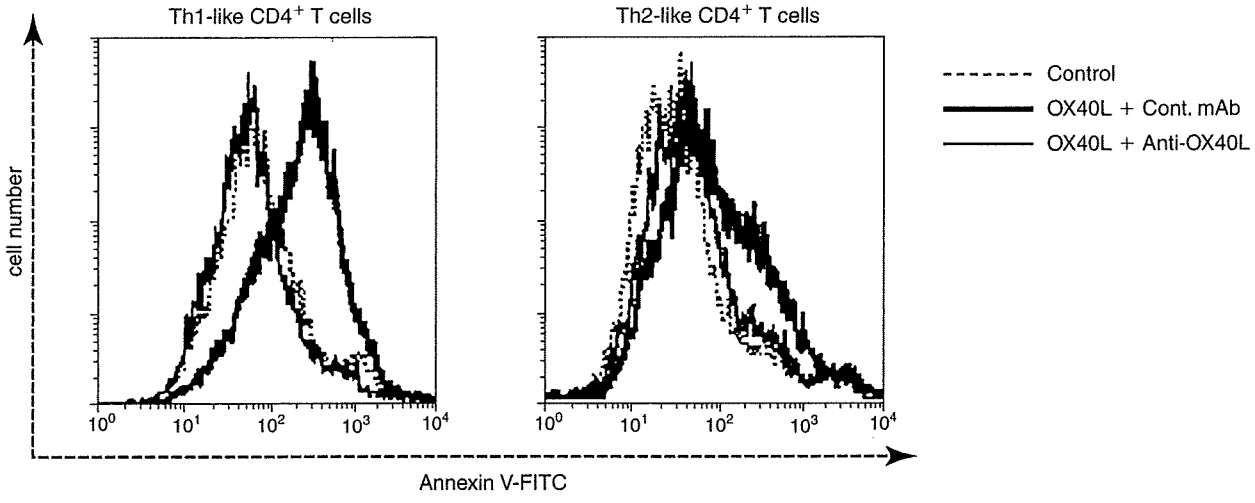


**FIG. 6.** Induction of apoptosis in primary activated $CD4^+$ T cells by cocultivation with OX40L-expressing cells. Two types of activated $CD4^+$ T cells from PBMCs of healthy donors, Th1-like and Th2-like, were activated in the presence of rhIL-12 and rhIL-4, respectively, on day 0, 3, and 6. After an additional 3 days, cells were cocultured with PFA-fixed SV-T2/OX40L (OX40L) or with PFA-fixed SV-T2/control (Control) cells in the presence of either anti-hOX40L blocking mAb (Anti-OX40L) or isotype control mAb (Cont. mAb). After 24 h, cells were stained by anti-hCD4-Cy5 and then stained by annexin V-FITC. Cells were analyzed with a FACSCalibur. Representative results from three independent experiments are shown.

OX40, M/R5-OX40del, and M/R5-control cells were stimulated with OX40L and/or TNF-$\alpha$, followed by the determination of cell viability using annexin V-FITC/PI staining. At 24 h following stimulation, apoptosis was apparent in M/R5-OX40 cells; however, no detectable apoptosis was observed in M/R5-OX40del cells (Fig. 4A), suggesting a signal from OX40 is indeed required for apoptosis. On the other hand, M/R5-OX40 cells pretreated with the broad-spectrum caspase inhibitor z-VAD-fmk and stimulated with OX40L, in the absence or presence of TNF-$\alpha$, were prevented from undergoing apoptosis (Fig. 4B), suggesting that the apoptosis was caspase cascade dependent. In accordance with this, Western blot assays showed that in OX40L-stimulated M/R5-OX40 cells, the levels of pre-caspase-8 (57 kDa) and pro-caspase-3 (32 kDa) were markedly reduced, and cleaved caspase-8 (43 kDa) was increased after OX40L stimulation (Fig. 4C). Taken together, these results indicate that the OX40-mediated apoptosis of M/R5-OX40 cells is dependent on both signaling via the cytoplasmic tail of OX40 and on the caspase cascade.

### *OX40-induced apoptosis in M/R5-OX40 cells is mediated by endogenous TNF-$\alpha$*

To explore the mechanisms involved in OX40-mediated apoptosis, M/R5-OX40 cells were examined in more detail, since these cells undergo apoptosis by OX40L stimulation without exogenous TNF. First, we examined the effects of various mAbs on OX40L-triggered cell death. As shown in Fig. 5A, anti-hTNF-$\alpha$ blocking mAb, but none of anti-hTNF-$\beta$, anti-hTRAIL, and anti-hFasL blocking mAbs, inhibited the cell death, showing that TNF-$\alpha$, but not TNF-$\beta$, TRAIL, and FasL, was involved in cell death after OX40L stimulation. Indeed, OX40L-stimulated M/R5-OX40 cells synthesized TNF-$\alpha$, which was detected in cell lysates, but not in culture supernatants (Fig. 5B). The fact that TNF-$\alpha$ was not detected in culture supernatants suggests that endogenously synthesized TNF-$\alpha$ bound to its membrane receptors (TNF-RI and/or TNF-RII) on the surface of cells stimulated with OX40L. The production of endogenous TNF-$\alpha$ was completely inhibited by anti-OX40L neutralizing mAb, showing that this endogenous TNF-$\alpha$ production was mediated by the OX40L/OX40 interaction (Fig. 5C). These results suggest that endogenous TNF-$\alpha$, induced by OX40 stimulation in the OX40$^+$ T cell line M/R5-OX40 mediates apoptosis. Furthermore, we also determined the induction of endogenous TNF-$\alpha$ in other OX40$^+$ cell lines. As shown in Fig. 5D, although endogenous TNF-$\alpha$ was induced in the T cell line CEM/OX40, it was not dependent on OX40L stimulation, unlike M/R5-OX40 cells. Interestingly, in another T cell line, Jurkat/OX40, endogenous TNF-$\alpha$ was not detected. On the other hand, two promonocytic cell lines, U937/OX40 and THP-1/OX40, strongly expressed endogenous TNF-$\alpha$ regardless of OX40 stimulation. The B cell line BJAB/OX40 also weakly expressed endogenous TNF-$\alpha$ regardless of OX40 stimulation. In all of these cell lines, soluble TNF-$\alpha$ was not detected in the culture supernatants after OX40L stimulation (data not shown).

### *Apoptosis of primary CD4$^+$ T cells by cocultivation with OX40L-expressing cells*

Finally, we determined whether apoptosis can be induced in primary CD4$^+$ T cells by OX40-stimulation *in vitro*. We generated two types of activated CD4$^+$ T cells from PBMCs of healthy donors, Th1-like and Th2-like, which were activated in the presence of IL-12 and IL-4, respectively. The Th1-like CD4$^+$ T cells expressed higher levels of functional OX40 than the Th2-like CD4$^+$ T cells.[45] These two types of cells were cocultured for 24 h with PFA-fixed SV-T2/OX40L or with PFA-fixed SV-T2/control cells in presence of either anti-hOX40L blocking mAb or isotype control mAb. As shown in Fig. 6, OX40 stimulation increased the levels of annexin V binding, especially in the Th1-like CD4$^+$ T cells. Since anti-OX40L mAb inhibited annexin V staining, these results suggest that under Th1-like conditions some fractions of primary CD4$^+$ T cells undergo apoptosis following OX40 stimulation.

## DISCUSSION

We show here, for the first time, that combined OX40L and TNF stimulation leads OX40$^+$ T cell lines and primary CD4$^+$ T cells to undergo apoptosis. Apoptosis-inducing effects have been described for a number of HIV-1 proteins, including Env,[46] Tat,[47] Nef,[48] Vpr,[49] and Vpu.[50] Recently, Lenardo *et al.* have shown that HIV-1 can induce necrosis of CD4$^+$ T cells.[51] However, the data presented herein, using the OX40 transfectants of the HIV-1-negative T cell line Molt-4/CCR5, clearly demonstrate that OX40-mediated cell death is independent of apoptosis- or of necrosis-inducing effects of HIV-1 proteins.

Stimulation of other DD-lacking members of the TNF-R superfamily, including TNF-R2, CD27, CD30, and CD40, induces the death of tumor cells and of normal cells under certain conditions. One known mechanism for TNF-R2-, CD30-, and CD40-induced cell death is that receptor stimulation activates cells to produce endogenous membrane TNF, which stimulates the DD-containing TNF-R1 to induce cell death.[31] A second mechanism suggested for CD40-mediated cell death is an amplification of the Fas-dependent apoptosis pathway.[52] In this study, we show that apoptosis in M/R5-OX40 cells, induced by OX40 stimulation, was efficiently blocked by the caspase inhibitor z-VAD-fmk, and was also blocked by anti-TNF-$\alpha$ neutralizing mAb. Moreover, the apoptosis of OX40-stimulated M/R5-OX40 cells was associated with the induction of endogenous TNF-$\alpha$. These results suggest that the OX40-mediated apoptosis in M/R5-OX40 cells occurs indirectly, via a TNF/TNF-R system reminiscent of that mediated via TNF-R2, CD30, and CD40.

The response to coactivation by OX40L plus TNF-$\alpha$ in Jurkat/OX40 cells is also of great interest. In Jurkat/OX40 cells, apoptosis was not induced by soluble TNF-$\alpha$ or by OX40 stimulation and endogenous TNF-$\alpha$ was not induced by OX40 stimulation, unlike the results observed in M/R5-OX40 cells. However, rapid apoptosis was induced in Jurkat/OX40 cells by costimulation with OX40L plus TNF-$\alpha$. These results suggest a new aspect of OX40 function in the induction of apoptosis in this cell line upon costimulation with OX40L plus TNF-$\alpha$. The degree to which this mechanism contributes to OX40-induced apoptosis in other cell lines, such as M/R5-OX40, CEM/OX40, U937/OX40, and THP-1/OX40, is not currently known. On the other hand, U937/OX40 and THP-1/OX40 cells were relatively resistant, and BJAB/OX40 cells were completely resistant to the combined stimulation with OX40L and TNF-$\alpha$ (Fig. 3A). Since endogenous TNF-$\alpha$ is expressed in these cells irrespec-

tive of stimulation, these cells might have an endogenous mechanism to resist TNF-$\alpha$-induced apoptosis. Furthermore, since normal B cells and monocytic cells do not express OX40, it might be possible that they lack the machinery for OX40-mediated intracellular signaling, or are equipped with an, as yet, undetermined anti-OX40 signal. Further studies are required to define the mechanisms of such resistance. In addition, since apoptosis of CEM/OX40 cells following OX40L stimulation could not be completely inhibited by the caspase inhibitor z-VAD-fmk at concentrations up to 100 $\mu$M (data not shown), it is possible that OX40-induced cell death may include additional apoptotic pathways, which may depend upon the cell line being studied.

It can be speculated that the survival or the apoptotic fate of $CD4^+$ T cells, after OX40 stimulation, is dependent on immunological environments. Kawamata *et al.* have shown that the cytoplasmic tail of OX40 binds TRAF2 and TRAF5, leading to NF-$\kappa$B activation.[12] TRAF2 is required for the TNF-mediated activation of c-Jun N-terminal kinase (JNK) and of NF-$\kappa$B, which leads to the generation of antiapoptotic signals.[3] It has been shown that TRAF2 can trigger cell death in the presence of the receptor-interacting protein (RIP), whereas in the absence of RIP, TRAF2 activates NF-$\kappa$B.[53] RIP has also been implicated in caspase-8-independent necrosis.[54] Furthermore, Li *et al.* have shown that activation of TNF-R2 induces ubiquitination and proteasomal degradation of TRAF2, leading to the enhancement of TNF-induced apoptosis.[55] In addition, it has been demonstrated that stimulation of TNF-R2, CD30, or CD40 leads to selective enhancement of TNF-R1-mediated caspase-8-dependent cell death by depletion of both TRAF2 and the antiapoptotic IAP proteins.[37] Another suggested mechanism for CD40L-mediated $CD4^+$ T cell death is failure of the induction of the antiapoptotic proteins Bcl-2 and Bcl-$X_L$.[56] However, this mechanism cannot explain OX40-mediated apoptosis, since OX40 activation has been shown to induce these two antiapoptotic proteins.[57] Recently, Ma *et al.* have shown that in both OX40 and 4-1BB-expressing cells, combined stimulation by OX40 and 4-1BB induces reduced NF-$\kappa$B activation, cell survival, and cell growth.[58] At present, it remains unclear whether OX40 activation directly mediates cell death. Taken together, it is interesting to speculate that OX40 stimulation induces cell death via an apoptotic pathway mediated by its cytoplasmic tail. Further studies are in progress to reveal the precise molecular mechanisms of OX40-induced apoptosis of T cells in various immunological environments.

In conclusion, the present study revealed a novel immunological function of OX40 in OX40-expressing $CD4^+$ T cells, with the control of cell death, in the presence of TNF, potentially resulting in a reduction of HIV-1 production.

## ACKNOWLEDGMENTS

This work was supported by grants from the Ministry of Education, Culture, Sports, Science and Technology of Japan, and the Ministry of Health, Labor and Welfare of Japan. We are grateful to Dr. A.A. Ansari (Emory University) for critical reading of this manuscript, Dr. H. Niwa (RIKEN) for the gift of the pCAGIPuro vector, and Dr. M. Baba (Kagoshima University) for the gift of the Molt-4/CCR5 cell line.

## REFERENCES

1. Latza U, Durkop H, Schnittger S, *et al.*: The human OX40 homolog: cDNA structure, expression and chromosomal assignment of the ACT35 antigen. Eur J Immunol 1994;24:677–683.
2. Mallett S, Fossum S, and Barclay AN: Characterization of the MRC OX40 antigen of activated CD4 positive T lymphocytes: A molecule related to nerve growth factor receptor. EMBO J 1990;9:1063–1068.
3. Baker SJ and Reddy EP: Modulation of life and death by the TNF receptor superfamily. Oncogene 1998;17:3261–3270.
4. Tanaka Y, Inoi T, Tozawa H, Yamamoto N, and Hinuma Y: A glycoprotein antigen detected with new monoclonal antibodies on the surface of human lymphocytes infected with human T-cell leukemia virus type-I (HTLV-I). Int J Cancer 1985;36:549–555.
5. Miura S, Ohtani K, Numata N, *et al.*: Molecular cloning and characterization of a novel glycoprotein, gp34, that is specifically induced by the human T-cell leukemia virus type I transactivator p40tax. Mol Cell Biol 1991;11:1313–1325.
6. Baum PR, Gayle RB 3rd, Ramsdell F, *et al.*: Molecular characterization of murine and human OX40/OX40 ligand systems: Identification of a human OX40 ligand as the HTLV-1-regulated protein gp34. EMBO J 1994;13:3992–4001.
7. Ohshima Y, Tanaka Y, Tozawa H, Takahashi Y, Maliszewski C, and Delespesse G: Expression and function of OX40 ligand on human dendritic cells. J Immunol 1997;159:3838–3848.
8. Stuber E, Neurath M, Calderhead D, Fell HP, and Strober W: Cross-linking of OX40 ligand, a member of the TNF/NGF cytokine family, induces proliferation and differentiation in murine splenic B cells. Immunity 1995;2:507–521.
9. Morimoto S, Kanno Y, Tanaka Y, *et al.*: CD134L engagement enhances human B cell Ig production: CD154/CD40, CD70/CD27, and CD134/CD134L interactions coordinately regulate T cell-dependent B cell responses. J Immunol 2000;164:4097–4104.
10. Imura A, Hori T, Imada K, *et al.*: The human OX40/gp34 system directly mediates adhesion of activated T cells to vascular endothelial cells. J Exp Med 1996;183:2185–2195.
11. Baba E, Takahashi Y, Lichtenfeld J, *et al.*: Functional CD4 T cells after intercellular molecular transfer of OX40 ligand. J Immunol 2001;167:875–883.
12. Kawamata S, Hori T, Imura A. Takaori-Kondo A, and Uchiyama T: Activation of OX40 signal transduction pathways leads to tumor necrosis factor receptor-associated factor (TRAF) 2- and TRAF5-mediated NF-kappa B activation. J Biol Chem 1998;273:5808–5814.
13. Flynn S, Toellner FM, Raykundalia C, Goodall M, and Lane P: CD4 T cell cytokine differentiation: The B cell activation molecule, OX40 ligand, instructs CD4 T cells to express interleukin 4 and upregulates expression of the chemokine receptor, Blr-1. J Exp Med 1998;188:297–304.
14. Ohshima Y, Yang LP, Uchiyama T, *et al.*: OX40 costimulation enhances interleukin-4 (IL-4) expression at priming and promotes the differentiation of naive human CD4(+) T cells into high IL-4-producing effectors. Blood 1998;92:3338–3345.
15. Akiba H, Miyahira Y, Atsuta M, *et al.*: Critical contribution of OX40 ligand to T helper cell type 2 differentiation in experimental leishmaniasis. J Exp Med 2000;191:375–380.
16. Tanaka H, Demeure CE, Rubio M, Delespesse G, and Sarfati M: Human monocyte-derived dendritic cells induce naive T cell differentiation into T helper cell type 2 (Th2) or Th1/Th2 effectors. Role of stimulator/responder ratio. J Exp Med 2000;192:405–412.
17. Gramaglia I, Jember A, Pippig SD, Weinberg AD, Killeen N, and Croft M: The OX40 costimulatory receptor determines the development of CD4 memory by regulating primary clonal expansion. J Immunol 2000;165:3043–3050.

18. De Smedt T, Smith J, Baum P, Fanslow W, Butz E, and Maliszewski C: OX40 costimulation enhances the development of T cell responses induced by dendritic cells in vivo. J Immunol 2002;168:661–670.
19. Bansal-Pakala P, Jember AJ, and Croft M: Signaling through OX40 (CD134) breaks peripheral T-cell tolerance. Nat Med 2001;7:907–912.
20. Valzasina B, Guiducci C, Dislich H, Killeen N, Weinberg AD, and Colombo MP: Triggering of OX40 (CD134) on CD4(+)CD25+ T cells blocks their inhibitory activity: A novel regulatory role for OX40 and its comparison with GITR. Blood 2005;105:2845–2851.
21. Imura A, Hori T, Imada K, *et al.*: OX40 expressed on fresh leukemic cells from adult T-cell leukemia patients mediates cell adhesion to vascular endothelial cells: Implication for the possible involvement of OX40 in leukemic cell infiltration. Blood 1997;89: 2951–2958.
22. Brocker T, Gulbranson-Judge A, Flynn S, Riedinger M, Raykundalia C, and Lane P: CD4 T cell traffic control: In vivo evidence that ligation of OX40 on CD4 T cells by OX40-ligand expressed on dendritic cells leads to the accumulation of CD4 T cells in B follicles. Eur J Immunol 1999;29:1610–1616.
23. Aten J, Roos A, Claessen N, Schilder-Tol EJM, Ten Berge IJM, and Weening JJ: Strong and selective glomerular localization of CD134 ligand and TNF receptor-1 in proliferative lupus nephritis. J Am Soc Nephrol 2000;11:1426–1438.
24. Ndhlovu LC, Ishii N, Murata K, Sato T, and Sugamura K: Involvement of OX40 ligand signals in the T cell priming events during experimental autoimmune encephalomyelitis. J Immunol 2001; 167:2991–2999.
25. Murata K, Nose M, Ndhlovu LC, Sato T, Sugamura K, and Ishii N: Constitutive OX40/OX40 ligand interaction induces autoimmune-like diseases. J Immunol 2002;169:4628–4636.
26. Jember AG-H, Zuberi R, Liu FT, and Croft M: Development of allergic inflammation in a murine model of asthma is dependent on the costimulatory receptor OX40. J Exp Med 2001;193:387–392.
27. Arestides RS, He H, Westlake RM, *et al.*: Costimulatory molecule OX40L is critical for both Th1 and Th2 responses in allergic inflammation. Eur J Immunol 2002;32:2874–2880.
28. Uchiyama T: Human T cell leukemia virus type I (HTLV-I) and human diseases. Annu Rev Immunol 1997;15:15–37.
29. Kopf M, Ruedl C, Schmitz N, *et al.*: OX40-deficient mice are defective in Th cell proliferation but are competent in generating B cell and CTL responses after virus infection. Immunity 1999;11: 699–708.
30. Ekkens MJ, Liu Z, Liu Q, *et al.*: The role of OX40 ligand interactions in the development of the Th2 response to the gastrointestinal nematode parasite Heligmosomoides polygyrus. J Immunol 2003;170:384–393.
31. Grell M, Zimmermann G, Gottfried E, *et al.*: Induction of cell death by tumour necrosis factor (TNF) receptor 2, CD40 and CD30: A role for TNF-R1 activation by endogenous membrane-anchored TNF. EMBO J 1999;18:3034–3043.
32. Prasad KV, Ao Z, Yoon Y, *et al.*: CD27, a member of the tumor necrosis factor receptor family, induces apoptosis and binds to Siva, a proapoptotic protein. Proc Natl Acad Sci USA 1997;94:6346–6351.
33. Mir SS, Richter BW, and Duckett CS: Differential effects of CD30 activation in anaplastic large cell lymphoma and Hodgkin disease cells. Blood 2000;96:4307–4312.
34. Lee SY, Park CG, and Choi Y: T cell receptor-dependent cell death of T cell hybridomas mediated by the CD30 cytoplasmic domain in association with tumor necrosis factor receptor-associated factors. J Exp Med 1996;183:669–674.
35. Hess S and Engelmann H: A novel function of CD40: Induction of cell death in transformed cells. J Exp Med 1996;183:159–167.
36. Chan FK and Lenardo MJ: A crucial role for p80 TNF-R2 in amplifying p60 TNF-R1 apoptosis signals in T lymphocytes. Eur J Immunol 2000;30:652–660.
37. Fotin-Mleczek M, Henkler F, Samel D, *et al.*: Apoptotic crosstalk of TNF receptors: TNF-R2-induces depletion of TRAF2 and IAP proteins and accelerates TNF-R1-dependent activation of caspase-8. J Cell Sci 2002;115:2757–2770.
38. Takahashi Y, Tanaka Y, Yamashita A, Koyanagi Y, Nakamura M, and Yamamoto N: OX40 stimulation by gp34/OX40 ligand enhances productive human immunodeficiency virus type 1 infection. J Virol 2001;75:6748–6757.
39. Biswas P, Smith CA, Goletti D, Hardy EC, Jackson RW, and Fauci AS: Cross-linking of CD30 induces HIV expression in chronically infected T cells. Immunity 1995;2:587–596.
40. Tozawa H, Andoh S, Takayama Y, *et al.*: Species-dependent antigenicity of the 34-kDa glycoprotein found on the membrane of various primate lymphocytes transformed by human T-cell leukemia virus type-I (HTLV-I) and simian T-cell leukemia virus (STLV-I). Int J Cancer 1988;41:231–238.
41. Tanaka Y, Yoshida A, Tozawa H, Shida H, Nyunoya H, and Shimotohno K: Production of a recombinant human T-cell leukemia virus type-I trans-activator (tax1) antigen and its utilization for generation of monoclonal antibodies against various epitopes on the tax1 antigen. Int J Cancer 1991;48:623–630.
42. Baba M, Miyake H, Okamoto M, Iizawa Y, and Okonogi K: Establishment of a CCR5-expressing T-lymphoblastoid cell line highly susceptible to R5 HIV type 1. AIDS Res Hum Retroviruses 2000;16:935–941.
43. Adachi A, Gendelman HE, Koenig S, *et al.*: Production of acquired immunodeficiency syndrome-associated retrovirus in human and nonhuman cells transfected with an infectious molecular clone. J Virol 1986;59:284–291.
44. Tanaka R, Yoshida A, Murakami T, *et al.*: Unique monoclonal antibody recognizing the third extracellular loop of CXCR4 induces lymphocyte agglutination and enhances human immunodeficiency virus type 1-mediated syncytium formation and productive infection. J Virol 2001;75:11534–11543.
45. Kondo K, Okuma K, Tanaka R, *et al.*: Requirements for the functional expression of OX40 ligand on human activated $CD4^+$ and $CD8^+$ T cells. Hum Immunol 2007;68:563–571.
46. Ohagen A, Ghosh S, He J, *et al.*: Apoptosis induced by infection of primary brain cultures with diverse human immunodeficiency virus type 1 isolates: Evidence for a role of the envelope. J Virol 1999;73:897–906.
47. Bartz SR and Emerman M: Human immunodeficiency virus type 1 Tat induces apoptosis and increases sensitivity to apoptotic signals by up-regulating FLICE/caspase-8. J Virol 1999;73:1956–1963.
48. Xu X-N, Laffert B, Screaton GR, *et al.*: Induction of Fas ligand expression by HIV involves the interaction of Nef with the T cell receptor zeta chain. J Exp Med 1999;189:1489–1496.
49. Hrimech M, Yao XJ, Bachand F, Rougeau N, and Cohen EA: Human immunodeficiency virus type 1 (HIV-1) Vpr functions as an immediate-early protein during HIV-1 infection. J Virol 1999;73: 4101–4109.
50. Casella CR, Rapaport EL, and Finkel TH: Vpu increases susceptibility of human immunodeficiency virus type 1-infected cells to fas killing. J Virol 1999;73:92–100.
51. Lenardo MJ, Angleman SB, Bounkeua V, *et al.*: Cytopathic killing of peripheral blood CD4 (+) T lymphocytes by human immunodeficiency virus type 1 appears necrotic rather than apoptotic and does not require env. J Virol 2002;76:5082–5093.
52. Afford SC, Ahmed-Choudhury J, Randhawa S, *et al.*: CD40 activation-induced, Fas-dependent apoptosis and NF-kappaB/AP-1 signaling in human intrahepatic biliary epithelial cells. FASEB J 2001;15:2345–2354.

53. Pimentel-Muinos FX and Seed B: Regulated commitment of TNF receptor signaling: A molecular switch for death or activation. Immunity 1999;11:783–793.
54. Holler N, Zaru R, Micheau O, *et al.*: Fas triggers an alternative, caspase-8-independent cell death pathway using the kinase RIP as effector molecule. Nat Immunol 2000;1:489–495.
55. Li X, Yang Y, and Ashwell JD: TNF-RII and c-IAP1 mediate ubiquitination and degradation of TRAF2. Nature 2002;416:345–347.
56. Blair PJ, Riley JL, Harlan DM, *et al.*: CD40 ligand (CD154) triggers a short-term CD4(+) T cell activation response that results in secretion of immunomodulatory cytokines and apoptosis. J Exp Med 2000;191:651–660.
57. Rogers PR, Son J, Gramaglia I, Killeen N, and Croft M: OX40 promotes Bcl-xL and Bcl-2 expression and is essential for long-term survival of CD4 T cells. Immunity 2001;15:445–455.
58. Ma BY, Mikolajczak SA, Danesh A, *et al.*: The expression and the regulatory role of OX40 and 4-1BB heterodimer in activated human T cells. Blood 2005;106:2002–2010.

Address reprint requests to:
*Yuetsu Tanaka*
*Department of Immunology*
*Graduate School of Medicine*
*University of the Ryukyus*
*Uehara 207*
*Nishihara, Okinawa 903-0215, Japan*

*E-mail:* yuetsu@s4.dion.ne.jp

# Overexpressed NF-κB–inducing kinase contributes to the tumorigenesis of adult T-cell leukemia and Hodgkin Reed-Sternberg cells

Yasunori Saitoh,[1] Norio Yamamoto,[1] M. Zahidunnabi Dewan,[1] Haruyo Sugimoto,[1] Vicente J. Martinez Bruyn,[1] Yuki Iwasaki,[1] Katsuyoshi Matsubara,[1] Xiaohua Qi,[1] Tatsuya Saitoh,[2] Issei Imoto,[3] Johji Inazawa,[3] Atae Utsunomiya,[4] Toshiki Watanabe,[5] Takao Masuda,[6] Naoki Yamamoto,[1,7] and Shoji Yamaoka[1]

[1]Department of Molecular Virology, Graduate School of Medicine, Tokyo Medical and Dental University, Tokyo; [2]Department of Host Defense, Research Institute for Microbial Diseases, Osaka University, Suita; [3]Department of Molecular Cytogenetics, Medical Research Institute and School of Biomedical Science, Tokyo Medical and Dental University, Tokyo; [4]Department of Hematology, Imamura Bun-in Hospital, Kagoshima; [5]Department of Medical Genome Sciences, Graduate School of Frontier Sciences, University of Tokyo, Tokyo; [6]Department of Immunotherapeutics, Graduate School of Medicine, Tokyo Medical and Dental University, Tokyo; and [7]AIDS Research Center, National Institute of Infectious Diseases, Tokyo, Japan

**The nuclear factor-κB (NF-κB) transcription factors play important roles in cancer development by preventing apoptosis and facilitating the tumor cell growth. However, the precise mechanisms by which NF-κB is constitutively activated in specific cancer cells remain largely unknown. In our current study, we now report that NF-κB–inducing kinase (NIK) is overexpressed at the pretranslational level in adult T-cell leukemia (ATL) and Hodgkin Reed-Sternberg cells (H-RS) that do not express viral regulatory proteins. The overexpression of NIK causes cell transformation in rat fibroblasts, which is abolished by a super-repressor form of IκBα. Notably, depletion of NIK in ATL cells by RNA interference reduces the DNA-binding activity of NF-κB and NF-κB–dependent transcriptional activity, and efficiently suppresses tumor growth in NOD/SCID/γc$^{null}$ mice. These results indicate that the deregulated expression of NIK plays a critical role in constitutive NF-κB activation in ATL and H-RS cells, and suggest also that NIK is an attractive molecular target for cancer therapy. (Blood. 2008;111:5118-5129)**



## Introduction

The nuclear factor-κB (NF-κB) transcription factors are known to regulate the expression of a wide range of genes involved in development, immune responses, apoptosis, and carcinogenesis as dimers of the REL family members, RelA, RelB, c-Rel, p50, and p52.[1] The p50 and p52 proteins are generated by proteasome-mediated processing of their precursors, p105 and p100, respectively. In resting cells, Rel proteins are sequestered in the cytoplasm through their interactions with the ankyrin repeats of the inhibitory proteins IκBα, -β, and -ϵ, as well as the precursor proteins p105 and p100. On stimulation, signals converge at the multiprotein IκB kinase (IKK) complex, which is composed of 2 catalytic subunits, IKK1/α and IKK2/β, and the scaffolding proteins, NF-κB essential modulator (NEMO, also known as IKKγ) and ELKS.[2] Phosphorylation by the IKK complex of specific serine residues on the IκB or precursor proteins results in their poly-ubiquitination and proteasome-dependent degradation or processing.[2] Released NF-κB then translocates to the nucleus and regulates expression of target genes.

NF-κB signaling pathways are largely classified as either canonical or noncanonical based on the stimuli and targets of the IKK complex.[2] Canonical activation is induced by stimuli, such as tumor necrosis factor-α (TNFα) and interleukin-1β, and involves NEMO- and IKK2/β-dependent phosphorylation and the subsequent degradation of IκB proteins. Noncanonical NF-κB pathways are activated after the stimulation of a range of TNF receptor family members, such as B-cell activating factor belonging to the TNF family (BAFF) receptor, lymphotoxin-β receptor, Fn14 and CD40, and direct NF-κB–inducing kinase (NIK)- and IKK1/α-dependent phosphorylation and subsequent processing of p100, leading to activation of NF-κB complexes containing RelB.[2,3] Of note in this context, the noncanonical pathways operate in a delayed fashion and are sensitive to protein synthesis inhibition.[4,5]

Compared with the mechanisms underlying the transduction of ligand-induced signaling to NF-κB activation, much less is known about how NF-κB is constitutively activated in a variety of cancer cells.[6] Constitutively high NF-κB activity has typically been demonstrated in human hematopoietic cancer cells, including adult T-cell leukemia (ATL), Hodgkin lymphoma, and multiple myeloma cells.[7,8] We have previously reported the aberrant expression of p52 in ATL and Hodgkin Reed-Sternberg (H-RS) cells that do not express viral regulatory proteins, such as Tax of the human T-cell leukemia virus or latent membrane protein 1 of the Epstein-Barr virus.[9,10] In addition, IKK activation in ATL and H-RS cells was found to be sensitive to protein synthesis inhibition.[10,11] These results indicate that the noncanonical pathways of NF-κB activation operate in these cancer cells. Aberrant p52 expression has also been reported in other types of cancer cells, including breast,[12] prostate,[13] pancreas,[14] and colon.[15] However, the actual triggers of noncanonical NF-κB activation in these cancer cells remain largely unknown except for certain multiple myeloma cells that have mutations in the *NIK*, *TRAF3*, and related genes.[16,17]

Submitted September 10, 2007; accepted February 17, 2008. Prepublished online as *Blood* First Edition paper, February 27, 2008; DOI 10.1182/blood-2007-09-110635.

The online version of this article contains a data supplement.

The publication costs of this article were defrayed in part by page charge payment. Therefore, and solely to indicate this fact, this article is hereby marked "advertisement" in accordance with 18 USC section 1734.

NIK is a serine-threonine kinase that is an essential participant in the induction of the IKK1-dependent processing of p100 as well as IκB degradation in response to stimuli, such as CD70, CD40 ligand, and BAFF.[18] It has also been reported previously that the IKK complex is recruited to CD27 in a manner dependent on NIK function. However, the mechanism by which NIK activity is regulated thereafter was unknown until it was recently demonstrated that these stimuli protect basally translated endogenous NIK protein from proteasome-mediated degradation.[19,20] Liao et al reported that the interaction of NIK with TNF receptor–associated factor 3 (TRAF3) is responsible for the rapid degradation of NIK and that noncanonical NF-κB stimuli induce the degradation of TRAF3 and the elevation of NIK expression.[19] In a separate study, Qing et al have demonstrated that noncanonical NF-κB stimuli stabilize the NIK protein but do not modify its RNA expression or protein translation.[20] The findings of these studies explain the delay in triggering the noncanonical pathway and its high sensitivity to protein synthesis inhibition.

Because NIK is a central regulator of the noncanonical pathway of NF-κB activation, we have investigated in our current study how this kinase is regulated in hematopoietic cancer cells, in which IKK is constitutively activated in the absence of viral regulators.

## Methods

### Cell culture

ED40515(−),[21] ATL-43Tb(−),[22] and TL-Om1[23] are human T-cell leukemia virus type-I (HTLV-I)–infected T-cell lines established from the leukemic cells of ATL patients. The H-RS cell lines, HDLM-2, L428, and L540, were purchased from the German Collection of Micro-organisms and Cell Cultures (Braunschweig, Germany). CEM[24] and Jurkat[25] are HTLV-I–free human T-lymphoblastic leukemia cell lines. A human B-cell line, Romas RG69,[20] was a kind gift from Dr Gutian Xiao (State University of New Jersey, Piscataway, NJ). Primary leukemia cells derived from ATL patients were obtained under informed consent at Imamura Bun-in Hospital and supplied through the Joint Study on Predisposing Factors of ATL Development. The patients were diagnosed with ATL on the basis of clinical and hematologic features and the presence of antibodies to ATL-associated antigens in serum and of the HTLV-I proviral genome in the leukemia cells. Use of peripheral blood lymphocytes from ATL patients for research purposes was approved by the institutional review board of each institute. Peripheral blood mononuclear cells (PBMCs) derived from healthy donors were also obtained under informed consent. PBMCs were isolated from both ATL patients and healthy donors by density gradient separation with Ficoll-Plaque PLUS (Amersham Biosciences, Uppsala, Sweden). Cells were maintained in RPMI 1640 supplemented with 10% fetal bovine serum, 100 U/mL penicillin G, and 100 μg/mL streptomycin sulfate; 5R is a NEMO-deficient subline of the Rat-1 cell line and has been described previously.[26] B5 and h12 are sublines of Rat-1 and 5R, respectively, express the blasticidin deaminase gene under the control of an NF-κB–dependent promoter, and have also been described previously.[26,27] Plat-E packaging cells were described previously.[28] B5, h12, Plat-E, 293T cells, and mouse embryonic fibroblasts were maintained in Dulbecco modified Eagle medium supplemented with 10% fetal bovine serum, 100 U/mL penicillin G, and 100 μg/mL streptomycin sulfate. Anchorage-independent cell growth was examined essentially as described previously.[29] Images were captured using an inverted microscope (IX70, Olympus, Tokyo, Japan) and processed with Openlab 3.0.2 software (Improvision, Coventry, United Kingdom). Cells used in this study were all maintained at 37°C in air containing 5% $CO_2$.

### Virus infection and transfection

Plat-E cells were transfected with pMRX-HA-NIK-ires-puro, pMRX-HA-kd-NIK-ires-puro, or pMRX-HA-ires-puro (EV1) (Document S1, available on the *Blood* website; see the Supplemental Materials link at the top of the online article) using the calcium phosphate precipitation method. Culture supernatants were collected 48 hours after transfection and filtered. B5 and h12 cells were infected for 2 hours in the presence of 10 μg/mL polybrene. Infected cells were then cultured in medium containing 2 μg/mL puromycin, and cell clones were isolated. Rat fibroblasts expressing SR-IκBα or its empty control vector (EV2) were established essentially as described previously.[10] For production of lentiviruses, 293T cells were cotransfected with pCS-puro-Ctli, pCS-puro-NIKi-1, or pCS-puro-NIKi-2 (Document S1) together with the pCMVΔR8.2 packaging construct and pHCMV-VSV-G (kind gifts from Dr I.S.Y. Chen) using FuGENE 6 (Roche Applied Science, Indianapolis, IN). Culture supernatants were collected 48 hours after transfection and filtered. ED40515(−) and ATL-43Tb(−) cells were infected once or twice with 24 hours interval with these lentiviruses for 6 hours in the presence of 10 μg/mL polybrene. At 48 hours after the infection, cells were cultured in medium containing 2 μg/mL puromycin for an additional 48 hours. These infectants were subjected to immunoblotting, electrophoretic mobility shift assay (EMSA), and transient transfection with 2 μg of IgκCona-luc[30] and pEF1-LacZ[26] using DMRIE-C (Invitrogen, Carlsbad, CA) according to the manufacturer's instructions. Assays for luciferase and β-galactosidase were performed 48 hours after transfection by standard methods. Luciferase activity was normalized on the basis of β-galactosidase activity. The growth of lentivirus-infected cells was determined by the trypan blue staining method.

### Immunoprecipitation

For the immunoprecipitation of endogenous NIK, approximately $2 \times 10^7$ cells were lysed in buffer A (20 mM Tris-HCl, pH7.5, 0.5% Nonidet P-40, 150 mM NaCl supplemented with 1 μg/mL aprotinin, 1 μg/mL leupeptin, 0.57 mM phenylmethanesulphonylfluoride, 10 μM MG132, 10 μM MG115) followed by preclearing with purified rabbit IgG (Cedarlane Laboratories, Hornby, ON) and protein G-Sepharose beads (Pierce Biotechnology, Rockford, IL). After centrifugation at 14000 rpm for 3 minutes, supernatants were subjected to immunoprecipitation with purified nonimmune rabbit IgG or anti-NIK antibody (#4994) (Cell Signaling Technology, Danvers, MA). Immunoprecipitates were washed 3 times with TNT buffer (20 mM Tris-HCl, pH 7.5, 200 mM NaCl, and 1% Triton X-100). Endogenous NIK proteins were detected by immunoblotting with anti-NIK antibody (#4994). For the immunoprecipitation of HA-tagged NIK, 750 μg cell lysates prepared with buffer A was subjected to immunoprecipitation with anti-HA antibody (12CA5, a kind gift from Dr A. Israël, Institut Pasteur Paris, Paris, France). Immunoprecipitates were washed 3 times with TNT buffer. HA-tagged NIK proteins were detected by immunoblotting with anti-NIK antibody. For immunoprecipitation of endogenous IKK1/2, 1500 μg cell lysates prepared with buffer A were subjected to immunoprecipitation with anti-IKK1 monoclonal antibody (B78-1; BD PharMingen, San Diego, CA) or purified mouse IgG2b (MI10-104; Bethyl Laboratories, Montgomery, TX). Immunoprecipitates were washed 3 times with TNT buffer. Expression of endogenous proteins was detected by immunoblotting with antiphospho-IKK1/IKK2 (Ser180/Ser181) (#2681; Cell Signaling Technology), anti-IKK1 (H-744), or anti-IKK2 (H-470; Santa Cruz Biotechnology, Santa Cruz, CA) antibodies.

### Quantitative RT-PCR

Total RNA was extracted using Isogen reagents (Nippon Gene, Tokyo, Japan) according to the manufacturer's instructions. Quantitative RT-PCR amplifications were performed with 100 ng total RNA, 0.3 μM of each primer, and 0.25 μM TaqMan probe using an ABI-7700 Sequence Detector (Applied Biosystems, Foster City, CA): reverse transcription was performed at 48°C for 30 minutes, Taq DNA polymerase was activated at 95°C for 10 minutes, followed by 45 amplification cycles of 95°C for 15 seconds, and annealing and extension at 60°C for 1 minute. The *NIK*, *VEGF*, *ICAM-1*, and *MMP-9* mRNA levels were normalized based on the amount of *18S* ribosomal RNA determined simultaneously by the real-time RT-PCR.

### Mice and inoculation of cells

NOD/SCID/$\gamma c^{null}$ (NOG)[31] mice were purchased from the Central Institute for Experimental Animals (Kawasaki, Japan). All mice were maintained under specific pathogen-free conditions in the Animal Center of Tokyo Medical and Dental University (Tokyo, Japan). The Ethical Review Committee of the institute approved the experimental protocol. ED40515(−) cells expressing Ctli or NIKi-1 and -2 were washed twice with serum-free RPMI 1640 and resuspended in the same medium. Mice were anesthetized with ether and inoculated subcutaneously in the postauricular region with $5 \times 10^6$ cells per mouse, as described previously.[31] We measured tumor size and weight 2 weeks after cell inoculation.

### Statistics

Statistical significance was evaluated using a 2-tailed, unpaired Student's *t* test. *P* values less than .05 were considered to be significant.

## Results

### NIK is aberrantly expressed in both adult T-cell leukemia and Hodgkin Reed-Sternberg cells

The constitutive processing of p100 to p52 in ATL and H-RS cells[9,10] prompted us to examine whether NIK is aberrantly expressed in both established and primary ATL cells. Immunoblotting of whole-cell lysates prepared from ATL or H-RS cells did not show any detectable NIK signal (data not shown); however, when endogenous NIK was immunoprecipitated from approximately 20 million of these cells and subjected to immunoblotting, NIK was specifically detectable in anti-NIK immunoprecipitates from ATL and H-RS cells, but not from control cells, such as CEM and Jurkat (Figure 1A). Previous studies revealed that inhibition of the proteasome function allowed for detection of endogenous NIK in simple whole-cell lysates of B-cell lines.[19,20] Treatment of ED-40515(−) cells with the MG132 proteasome inhibitor for 3 hours before harvesting enabled us to observe robust endogenous NIK expression at the expected position (Figure 1B). Lysates of 293T cells with or without exogenous NIK expression were used as the positive and negative controls, respectively. We next examined the NIK expression levels as well as those of p100 phosphorylated at serine residues 866 and 870 in a panel of ATL, H-RS, and control cells (Figure 1C). No appreciable NIK expression could be observed in control CEM and Jurkat T-cell lines treated with MG132, in which NF-κB is not constitutively activated. Proteasome inhibition induced strong NIK expression in other Tax-negative ATL-derived cell lines, ATL-43Tb(−) and TL-Oml. Proteasome inhibition also strongly augmented NIK expression in H-RS cells, but only weakly so in the control B-cell lines, RG69. These results indicate that the steady-state levels of NIK of the authentic size are elevated in ATL and H-RS cells, and suggest that NIK may be abundantly produced in ATL and H-RS cells, but is rapidly degraded by the proteasome. The levels of NIK expression correlated well with those of phosphorylated p100 (Figure 1C). Moreover, p52 and the phoshorylated form of IκBα were also abundant in ATL and H-RS cell lines, but not in the control T-cell lines (Figure 1C). These results indicate that the overexpression of NIK is closely linked to the downstream events leading to constitutive activation of the canonical and noncanonical NF-κB pathways in ATL and H-RS cells. A previous study suggested that L428 cells express a C-terminally truncated form of IκBα and that the phosphorylated form of this protein was accumulated after treatment of the cells with proteasome inhibitor or dexamethasone.[32,33] In agreement with this, we did not detect IκBα expression with the antibody used in this study, which recognizes the C-terminus of the protein, but detected the phoshorylated form of this IκBα only after treatment with MG132 (data not shown).

We next investigated *NIK* expression at the mRNA level by quantitative PCR (Figure 1D) and found that that *NIK* transcripts were at between 20- and 100-fold higher levels in ATL and H-RS cells, compared with CEM cells. Next, actinomycin D was used to block new mRNA synthesis, so that decay of existing transcripts could be detected. Quantitative PCR analyses revealed that the half-life of *NIK* mRNA was approximately 3 hours both in the ATL and control T cells (Figure 1E). Essentially similar results were obtained with the other cell lines shown in Figure 1D, including H-RS cell lines (data not shown). A previous report has demonstrated that NF-κB is constitutively activated in primary ATL cells in the peripheral blood.[34] We therefore quantified the *NIK* mRNA levels in PBMCs from both healthy donors and ATL patients (Figure 2A), and found that *NIK* mRNA is overexpressed in PBMCs of 15 of 21 ATL patients. Actinomycin D treatment of PBMCs further revealed that *NIK* mRNA was not apparently stabilized in primary ATL cells (Figure 2B). Moreover, fluorescence in situ hybridization studies on primary ATL cells failed to detect amplification or translocation of the *NIK* gene (Figure S1; Table S2). Finally, when PBMCs were cultured for 3 hours in the presence of MG132, NIK protein was detectable in cells from an ATL patient showing abundant *NIK* mRNA expression, but not in those from a healthy donor (Figure 2C).

### NIK transforms rat fibroblasts in an NF-κB–dependent manner

To further explore the roles for NIK during cell transformation, we infected the 3T3-like rat fibroblast cell line Rat-1 with a retroviral vector expressing human NIK and examined its oncogenic activity. As expected, cells transduced with this NIK vector exhibited strong NF-κB DNA binding activity within 36 hours (data not shown). Rat-1 cells transduced with a control retrovirus became resistant to the selection marker puromycin approximately 24 hours after infection and continued to proliferate rapidly. In contrast, Rat-1 cells transduced with the NIK expression vector expressed a readily detectable level of NIK, had a transformed morphology, but ceased proliferating and died within 3 to 4 days after becoming resistant to puromycin. Cells that survived 2 weeks of puromycin selection after NIK transduction eventually appeared indistinguishable from those transduced with the control vector and showed no detectable NIK expression or NF-κB DNA binding activity (data not shown).

Based on these observations, we speculate that the retroviral overexpression of NIK is toxic to the cells so that only cells that had lost its expression could emerge from the puromycin-resistant pools. To address this problem, we used B5 and h12 cells carrying an integrated Igκ2bsrH plasmid that confers resistance to the antibiotic blasticidin S when cells are constitutively expressing active NF-κB.[26] B5 cells are derived from Rat-1 cells, and h12 cells are from 5R cells that lack NEMO expression. When the B5 and h12 cells were transduced with the wild-type NIK retroviral expression vector and subjected to selection with both puromycin and blasticidin S, the majority of the resultant cell clones maintained detectable NIK expression (Figure 3A), elevated catalytic activity of IKK (Figure 4), and the initial transformed morphology (Figure 5B). On the other hand, when B5 and h12 cells were transduced with a retrovirus vector expressing a catalytically inactive mutant form of NIK and selected with puromycin alone, the cells successfully

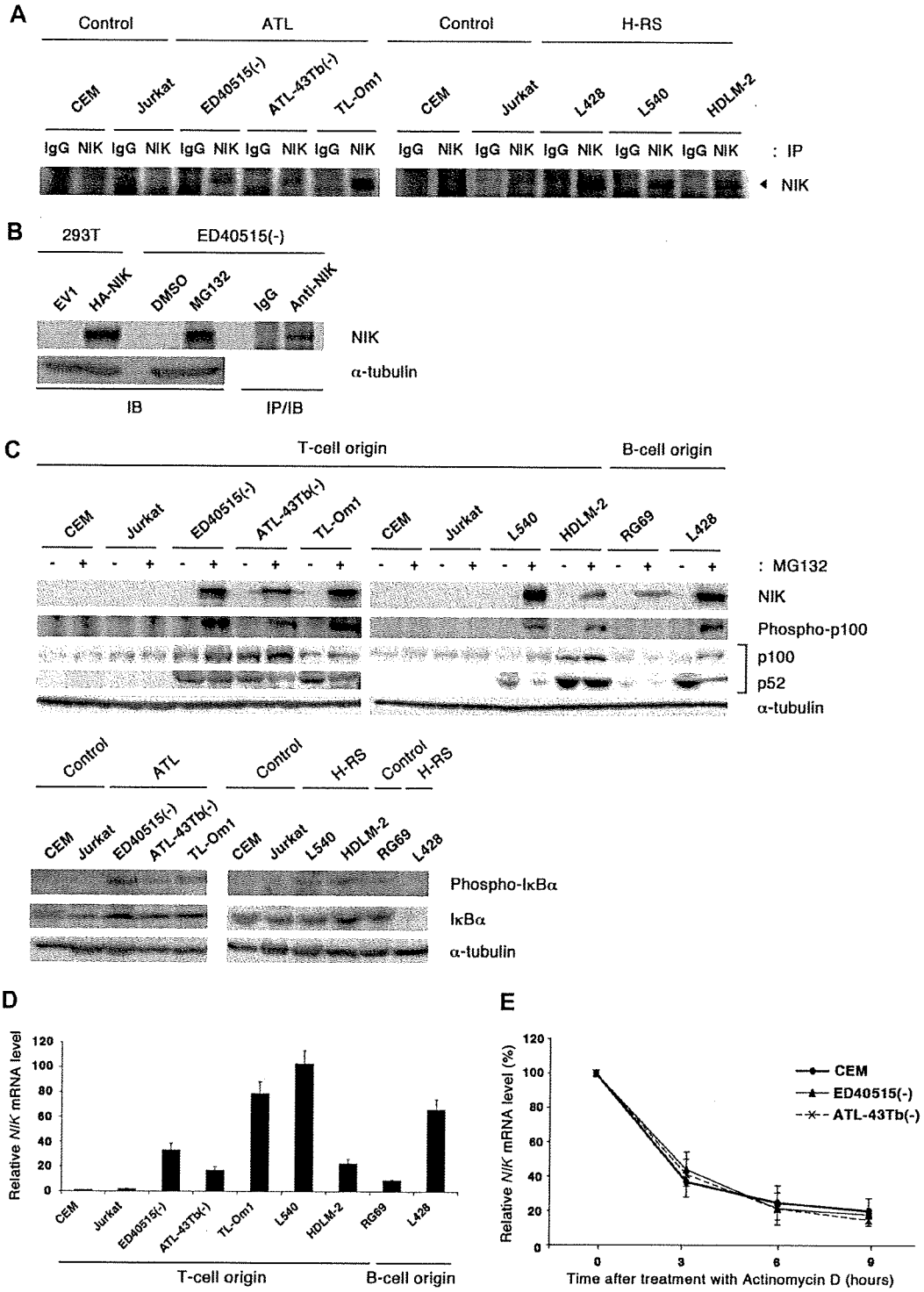


**Figure 1. NIK protein is overexpressed in established ATL and Hodgkin Reed-Sternberg cells.** (A) Steady-state levels of NIK expression in the ATL and H-RS cell lines were revealed by immunoprecipitation-coupled immunoblotting. Approximately $2 \times 10^7$ cells were lysed with buffer A. After preclearing, immunoprecipitation was performed at 4°C, using anti-NIK antibody (NIK) or its isotype IgG (IgG). After 3 washes with TNT buffer, immune complexes were analyzed by immunoblotting with anti-NIK antbody. (B) 293T cells were transfected with pMRX-HA-iresPuro or pMRX-HA-NIKiresPuro for 24 hours. Whole-cell lysates were used as negative and positive controls. ED40515(−) cells were pretreated with (+) or without (−) MG132 (20 μM) for 3 hours, lysed with RIPA buffer, and subjected to immunoblotting with anti-NIK or anti-α-tubulin antibodies. Immunoprecipitation-coupled immunoblotting was performed as in panel A. (C) Top panels: control T-cell lines (CEM and Jurkat), leukemic cell lines derived from ATL patients that do not express Tax(ED40515(−), ATL43-Tb(−), and TL-Om1, a control B-cell line (RG69), and H-RS cell lines (HDLM-2 and L540) were pretreated with (+) or without (−) MG132 (20 μM) for 3 hours, and 30 μg of the whole-cell extracts were subjected to Western blot analysis with the antibodies to the indicated proteins. Bottom panels: Whole-cell extracts from the indicated cell lines were analyzed by Western blotting with the antibodies to the indicated proteins. (D) Total RNA was extracted from the indicated cell lines and subjected to real-time RT-PCR to quantify the *NIK* mRNA levels. The *NIK* mRNA levels were normalized to *18S* RNA. The relative *NIK* mRNA levels shown represent the fold increases in mRNA abundance, relative to that of the CEM cells (arbitrarily set at 1). (E) Cells were cultured in the presence of actinomycin D (5 μg/mL) for the times indicated, and then total RNA was isolated and subjected to quantitative RT-PCR as in panel D. Data are expressed as mean plus or minus SD of 3 independent experiments. The relative amounts of *NIK* mRNA shown represent the percentages in mRNA abundance, relative to that of each cell line before the addition of actinomycin D (arbitrarily set at 100%). IB indicates immunoblotting; IP, immunoprecipitation.

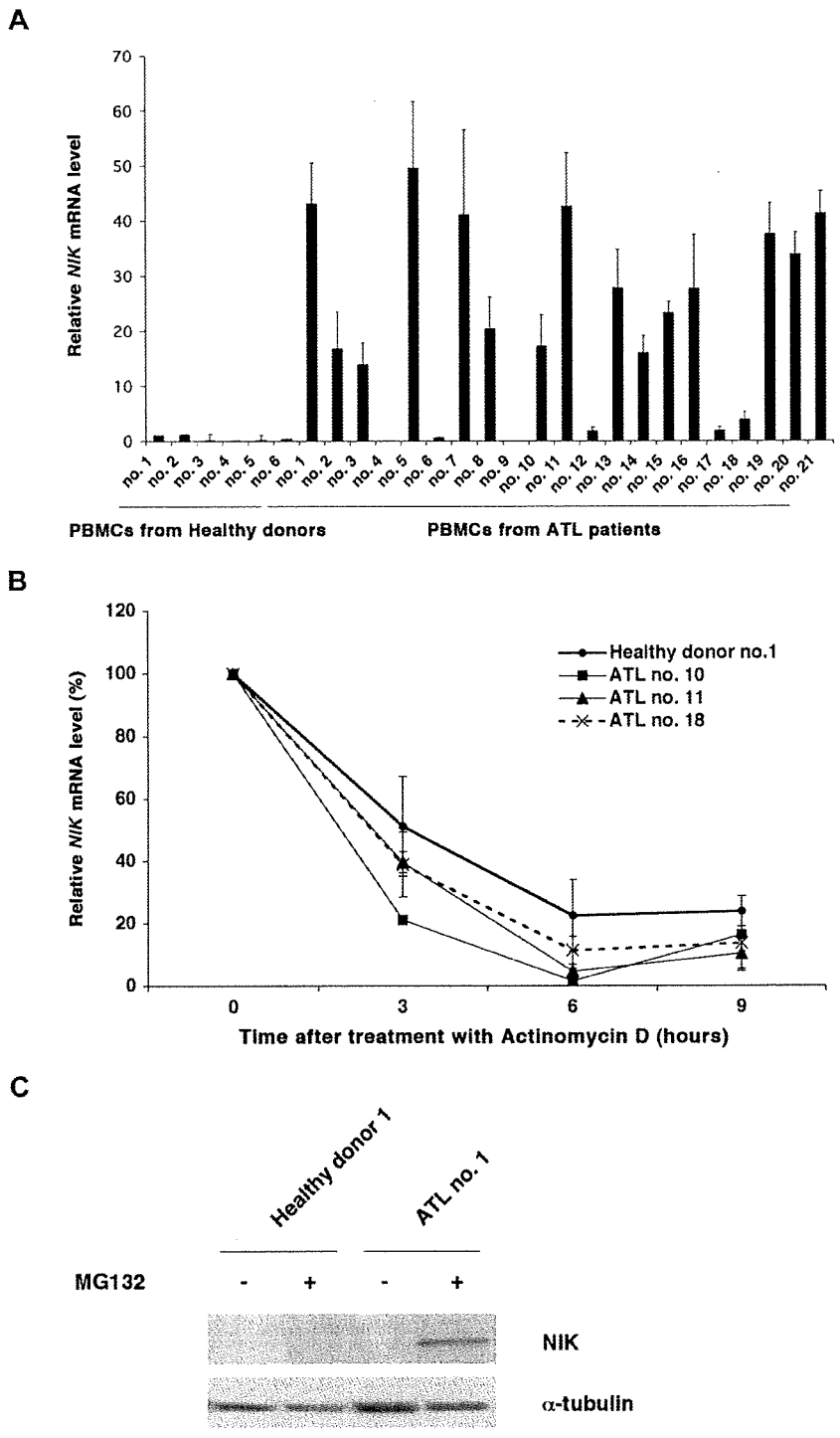


**Figure 2. Overexpression of the *NIK* mRNA and protein in PBMCs from ATL patients.** (A) Total RNA was extracted from PBMCs from healthy donors and ATL patients and then subjected to quantitative RT-PCR. The *NIK* mRNA levels were normalized to *18S* RNA. The relative *nik* mRNA levels shown represent the fold increases in mRNA abundance relative to that of healthy donor 1 (arbitrarily set at 1). These data are expressed as the mean plus or minus SD of 3 independent experiments. (B) PBMCs were cultured in the presence of actinomycin D (5 μg/mL) for the times indicated, and then total RNA was isolated and subjected to quantitative RT-PCR. The relative amounts of *NIK* mRNA shown represent the percentages in mRNA abundance, relative to that of PBMCs before the addition of actinomycin D (arbitrarily set at 100%). (C) PBMCs from a healthy donor and an ATL patient were treated with (+) or without (−) MG132 (20 μM) for 3 hours, lysed with RIPA buffer, and subjected to immunoblotting with anti-NIK or anti-α-tubulin antibodies.

expressed this protein (Figure 3A) without significant morphologic change (Figure 5B) or constitutive NF-κB activation (Figure 3C). As expected, these cells failed to survive selection with blasticidin S (data not shown).

The expression of wild-type NIK in B5 and h12 cells potently induces p52 expression and NF-κB DNA binding activity, whereas the catalytically inactive NIK mutant does not (Figure 3B,C). We also found a specifically phosphorylated form of IκBα in cells expressing wild-type NIK (Figure 3A). Super-shift experiments revealed that the NF-κB–DNA binding complexes in B5 and h12 cells expressing NIK involve p50, RelB, and RelA (Figure 4D). The presence of p52 in the DNA binding complexes could not be examined, however, because an antibody recognizing rat p52 in super-shift assay is not currently available. Instead, we analyzed DNA-binding complexes induced by NIK expression in wild-type mouse embryonic fibroblasts (Figure S2). Retroviral overexpression of NIK indeed induced DNA-binding NF-κB complexes containing p52, and enhanced expression of p52 and phosphorylated form of IκBα.

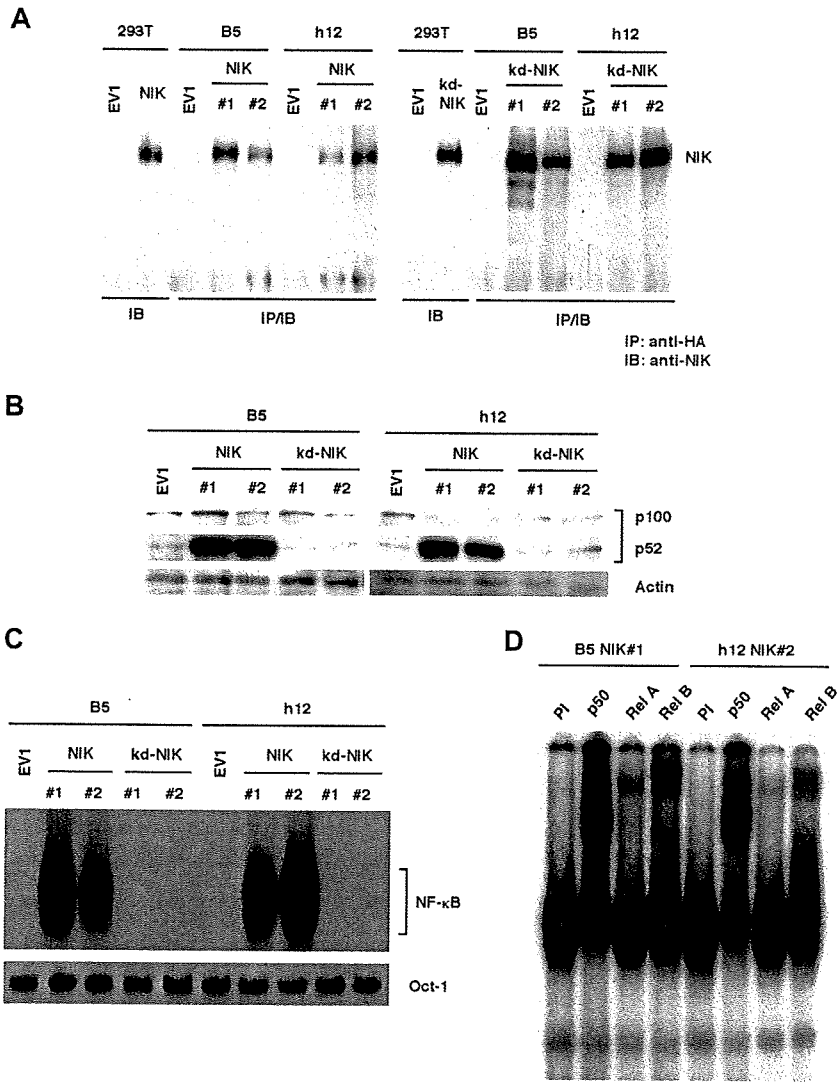


**Figure 3. NIK induces constitutive NF-κB activity in rat fibroblasts.** (A) B5 and h12 cells were infected with retroviruses capable of expressing HA-tagged NIK (NIK) or catalytically inactive NIK (kd-NIK). Pools of B5 and h12 cells transduced with the control pMRX-HAiresPuro vector (EV1) were used as a control. Cytoplasmic extracts from EV1 and 2 independent cell clones (no. 1 and no. 2) were subjected to immunoprecipitation using antibody against the HA epitope. Immunoprecipitates were then resolved by 8% SDS-PAGE and subjected to immunoblotting with anti-NIK antibody. 293T cells were transiently transfected with the pMRX-HAiresPuro vector (EV1) or pMRX-HA-NIKiresPuro (NIK). Cytoplasmic extracts (30 μg) were then used for immunoblotting as negative and positive controls, respectively. (B) Elevated p52 production in rat fibroblasts. Whole-cell lysates from B5 and h12 cells expressing wild-type NIK or kd-NIK were subjected to SDS-PAGE and immunoblotting with anti-p52 for detection of p100 and p52 or antiactin antibodies. (C) Elevated NF-κB–DNA binding activity in rat fibroblasts; 5 μg of nuclear extracts prepared from B5 and h12 cells expressing wild-type NIK or kd-NIK were analyzed by EMSA, using oligonucleotides encoding an NF-κB–binding sequence or Oct-1–binding sequence as probes. (D) DNA-binding NF-κB components in B5 and h12 cells expressing wild-type NIK were analyzed by super-shift EMSA. Nuclear extracts (5 μg) from B5 NIK#1 and h12 NIK#2 cells were preincubated for 30 minutes with preimmune (PI), anti-p50, anti-RelA or anti-RelB sera, and then subjected to EMSA with the NF-κB–specific probe. IB indicates immunoblotting; IP, immunoprecipitation.

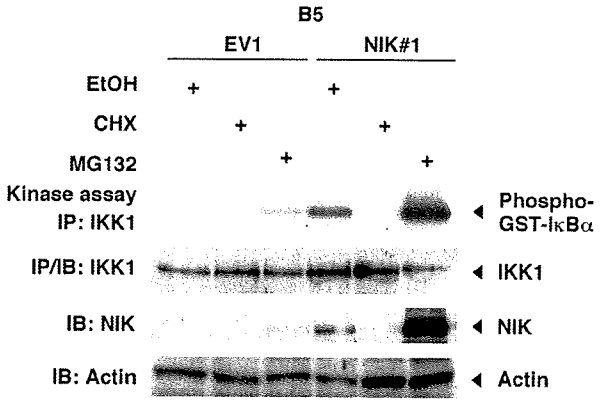


**Figure 4. NIK expression parallels IKK activity after CHX or MG132 treatment.** B5 cells transduced with the control vector (EV1) or B5 cells expressing wild-type NIK (NIK#1) were treated for 4 hours with either vehicle (ethanol, EtOH), cycloheximide (CHX; 50 μg/mL), or MG132 (20 μM). Cytoplasmic extracts were subjected to immunoprecipitation with IKK1-specific antibody, and then immunoprecipitates were used for an in vitro kinase assay. IKK1 expression in the immunoprecipitates was revealed by immunoblotting with IKK1-specific antibody. NIK and actin levels in the cytoplasmic extracts used for immunoprecipitation were determined by immunoblotting with anti-NIK or antiactin antibodies, respectively. IB indicates immunoblotting; IP, immunoprecipitation; GST, glutathione-S-transferase tag.

We have previously demonstrated that the treatment of ATL cells with MG132 greatly enhances IKK activity, whereas protein synthesis inhibition quickly abolished this activity.[11] Figure 4 shows that the IKK activity in B5 cells stably expressing NIK (NIK#1) is modulated by MG132 and cycloheximide (CHX) in a manner that is very similar to that seen in ATL cells. In addition, treatment of NIK#1 cells with MG132 remarkably elevates the level of exogenous NIK expression. The constitutive NF-κB activation caused by the presence of exogenous NIK was found to be abolished by the retroviral expression of a super-repressor form of IκBα (SR-IκBα), without affecting exogenous NIK expression (Figure 5A). Interestingly, the forced expression of SR-IκBα also diminishes the p52 and p100 expression levels.

We next tested the ability of NIK to induce anchorage-independent growth of rat fibroblasts. B5 and h12 cells transduced with the control vector did not form colonies of significant size in soft agar, whereas those transduced with wild-type NIK expression vector formed a number of large colonies, as shown in Figure 5B and Table 1. Cells expressing catalytically inactive NIK failed to form colonies in soft agar. The expression of SR-IκBα completely abolished NIK-induced colony formation and also the morphologic alterations of B5 and h12 cells. Given that SR-IκBα specifically suppresses NF-κB activation,

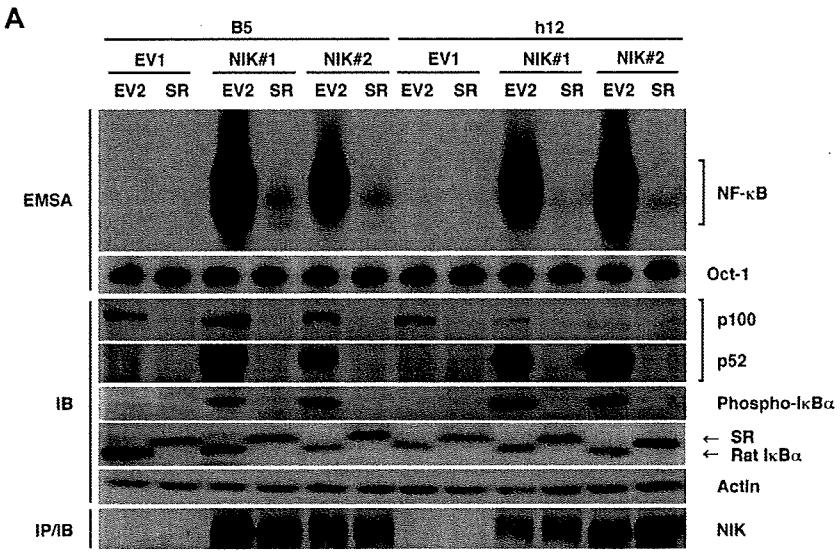


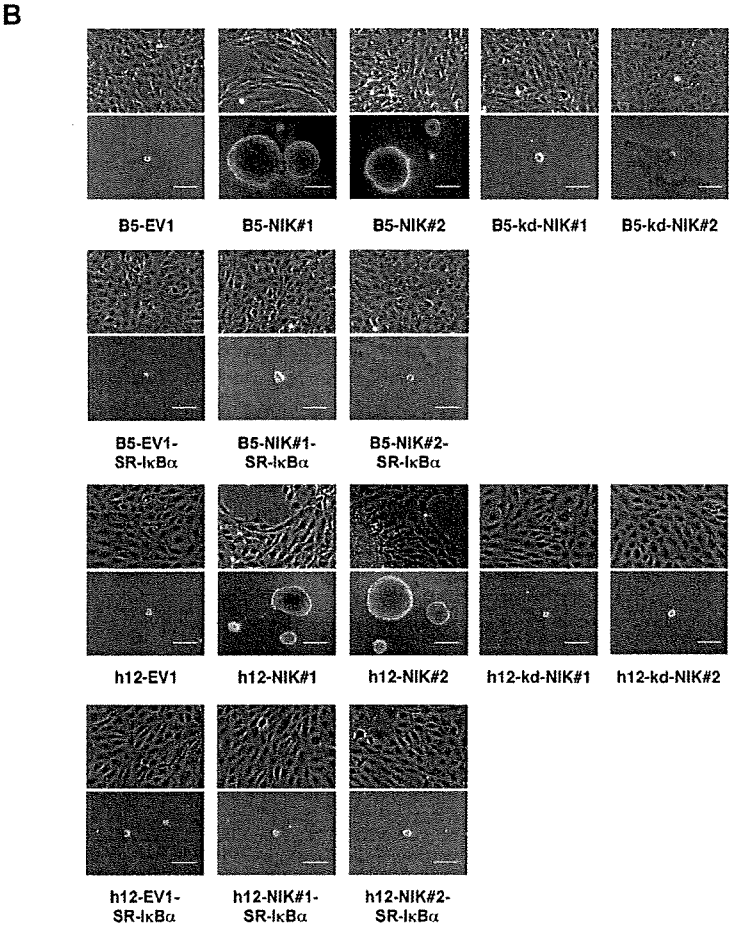


**Figure 5. The overexpression of NIK transforms rat fibroblasts in an NF-κB–dependent manner.** (A) Top 2 panels: 5 μg of nuclear extracts prepared from B5 and h12 cells transduced with empty vector (EV2) or SR-IκBα (SR) were analyzed by EMSA, using NF-κB and Oct-1 probes. Middle 5 panels: whole-cell extracts (30 μg) of B5 or h12 infectants were subjected to SDS-PAGE and immunoblotting with anti-p52, antiphospho-IκBα, anti-IκBα, or antiactin antibodies. Bottom panel: HA-tagged NIK was immunoprecipitated from B5 and h12 infectants with anti-HA antibody and detected by immunoblotting with anti-NIK antibody (H-248). (B) Phase-contrast micrographs of cells cultured on monolayers (top images) or in soft agar (bottom images). B5 or h12 cell clones expressing wild-type NIK (NIK#1 and NIK#2) or not (EV1) were cultured in soft agar for 3 weeks. These cells were further transduced with SR-IκBα, and then pooled cells were assayed for anchorage-independent growth in soft agar. B5 and h12 cell clones expressing kd-NIK were also examined. Original magnification ×100. Scale bar represents 100 μm. SR indicates super-repressor; kd-NIK, catalytically inactive NIK; IB, immunoblotting; IP, immunoprecipitation.

we conclude from these results that NIK transforms rat fibroblasts in an NF-κB–dependent manner.

### NIK mediates constitutive NF-κB activation in ATL cells

The similar modulation of IKK activity by CHX or MG132 in both ATL and B5 cells expressing NIK (Figure 4) suggests that NIK plays an important role in constitutive NF-κB activation in ATL cells. We therefore examined whether the RNA interference-mediated silencing of endogenous *NIK* gene expression would lower NF-κB–dependent transcription in these cells. ED-40515(−) and ATL-43Tb(−) cells were infected with lentiviral constructs that express short hairpin RNA (shRNA) molecules that target mRNA for either *Renilla luciferase* (Ctli) or *NIK* (NIKi), and then subjected to puromycin selection for 2 days. To

**Table 1. Efficiency of colony formation in soft agar**

| Cells* | Colony-forming efficiency, % | Average size of colonies, μm† |
|---|---|---|
| B5-EV1 | 0.7 ± 0.5 | 62.6 ± 1.5 |
| B5-NIK#1 | 23.2 ± 2.0‡ | 236.2 ± 12.6‡ |
| B5-NIK#2 | 18.9 ± 2.4‡ | 184.1 ± 19.8‡ |
| B5-kd-NIK#1 | 1.5 ± 0.3 | 63.1 ± 1.4 |
| B5-kd-NIK#2 | 1.3 ± 0.1 | 62.8 ± 1.8 |
| h12-EV1 | 1.2 ± 0.3 | 60.5 ± 0.0 |
| h12-NIK#1 | 12.8 ± 1.7‡ | 146.9 ± 4.6‡ |
| h12-NIK#2 | 17.7 ± 1.7‡ | 154.9 ± 5.6‡ |
| h12-kd-NIK#1 | 1.4 ± 1.0 | 61.5 ± 2.1 |
| h12-kd-NIK#2 | 1.5 ± 0.4 | 62.5 ± 4.7 |
| B5-EV1-EV2 | 1.2 ± 0.3 | 61.8 ± 1.1 |
| B5-NIK#1-EV2 | 21.1 ± 1.0‡ | 193.8 ± 3.7‡ |
| B5-NIK#2-EV2 | 14.3 ± 1.0‡ | 150.4 ± 8.7‡ |
| h12-EV1-EV2 | 1.5 ± 0.7 | 60.8 ± 0.4 |
| h12-NIK#1-EV2 | 12.3 ± 1.7‡ | 119.4 ± 5.6‡ |
| h12-NIK#2-EV2 | 14.0 ± 1.8‡ | 160.3 ± 7.2‡ |
| B5-EV1-SR-IκBα | 1.5 ± 0.0 | 61.7 ± 0.5 |
| B5-NIK#1-SR-IκBα | 3.4 ± 0.0 | 64.8 ± 1.1 |
| B5-NIK#2-SR-IκBα | 3.9 ± 0.1 | 63.3 ± 0.4 |
| h12-EV1-SR-IκBα | 1.7 ± 1.0 | 61.3 ± 0.4 |
| h12-NIK#1-SR-IκBα | 2.7 ± 0.3 | 62.3 ± 0.1 |
| h12-NIK#2-SR-IκBα | 3.4 ± 1.4 | 61.4 ± 0.2 |

kd-NIK indicates catalytically inactive NIK; SR, super-repressor; EV1, empty vector for NIK or kd-NIK; and EV2, empty vector for SR-IκBα.

*Cells were inoculated in 0.33% soft agar and cultured for 3 weeks.

†Colonies larger than 60 μm were counted as positive. The sizes of more than 100 positive colonies were averaged.

‡$P < .05$ vs B5-EV1.

suppress NIK expression maximally, we used independently or in combination 2 shRNAs (NIKi-1 and -2) that target different *NIK* sequences and reduce NIK expression. The infected cells were then assayed for transcriptional activity by transient transfection with an NF-κB–dependent reporter gene (Figure 6A). Lentiviral expression of NIKi constructs resulted in suppression of NF-κB–dependent reporter gene expression in ATL cells when independently used, and the combined use of the 2 NIKi constructs (NIKi-1 and -2) was found to be more effective. We then examined ATL cells transduced with NIKi-1 and -2 constructs for the expression of endogenous NIK and specifically phosphorylated forms of p100, IκBα, and IKKs by immunoblotting (Figure 6B) and for NF-κB DNA binding activity by EMSA (Figure 6C). NIK expression in ATL cells was found to be down-regulated by the shRNA-mediated silencing (Figure 6B). As expected, p52 and phosphorylated p100 were also reduced by NIK depletion, and interestingly, phoshorylation of IκBα was also suppressed. This is consistent with the results observed in NIK-transduced rat fibroblasts that express the phoshorylated form of IκBα (Figure 5A), indicating that NIK, when aberrantly and stably expressed, induces phosphorylation of IκBα. In addition, NIK depletion suppressed phosphorylation of the serine residues in the activation loop of IKKs, suggesting a key role for NIK in constitutive activation of IKKs in ATL cells (Figure 6B). Moreover, depletion of NIK resulted in suppression of NF-κB DNA binding activity (Figure 6C). Super-shift assays revealed that DNA-binding of NF-κB components, p50, p52, RelA, and RelB was reduced by NIK depletion (Figure 6D). As shown previously, c-Rel was not detected in ATL cells.[34] We further investigated alterations in the expression of NF-κB target genes by NIK depletion. Vascular endothelial growth factor (VEGF), matrix metalloproteinase-9 (MMP-9), and intracellular adhesion molecule-1 (ICAM-1), the expression of which has been reported to be under the control of NF-κB,[35-37] are highly expressed in ATL cells and suggested to contribute to their invasive properties.[38-41] Quantitative RT-PCR studies reveal that depletion of NIK results in down-regulation of the expression of these NF-κB target genes (Figure 6E).

### NIK regulates tumorigenicity of ATL cells in vivo

We finally investigated biologic effects of NIK depletion in ATL cells. NIK depletion did not significantly influence the growth of cells in culture (Figure 7A). We then examined whether depletion of NIK affects the tumorigenicity of ATL cells in a mouse model. NOD/SCID/$\gamma c^{null}$ mice were subcutaneously inoculated with ED-40515(−) cells that express Ctli or NIKi and are characterized in Figure 6B,C, and tumor formation was evaluated 2 weeks later. As expected, ED-40515(−) cells expressing Ctli efficiently formed large tumors, whereas tumors formed in mice inoculated with ED-40515(−) cells expressing NIKi were significantly smaller (Figure 7B-D), suggesting that NIK supports efficient tumor cell growth in vivo.

## Discussion

Persistent activation of NF-κB has previously been reported to play an essential role in the growth and survival of specific cancer cell types, including ATL, H-RS, melanoma, and prostate cancer cells.[9,42-45] Inappropriate NF-κB activation can also contribute to the resistance to the apoptotic responses induced by certain anticancer drugs.[46] On the other hand, cancer cell apoptosis can be induced when persistent NF-κB activity is blocked by inhibitors, such as SR-IκBα, by drugs targeting IKK or the proteasome, via peptides targeting p50 or NEMO, and by double-stranded oligonucleotides containing NF-κB binding sites.[47,48] One problem with such inhibitors, however, is their lack of specificity to cancer cells because they also necessarily block normal NF-κB activation. Hence, it would be desirable to specifically inhibit NF-κB activation in cancer cells by identifying molecular targets in each cancer type. Virally transformed cancer cells express a virus-derived regulatory protein(s) that targets critical molecules in a variety of key signaling pathways. Cytokine autocrine loops or genetic alterations to genes regulating the NF-κB signaling mechanisms that lead to persistent NF-κB activation have also been identified in some cancer cells.[16,17,32,47,49] However, the mechanisms underlying persistent NF-κB activation in many types of cancer remain unknown.

Most primary ATL cells, although infected with HTLV-I, are characterized by the loss of viral protein expression, including Tax, probably because of the host immune surveillance during the long period of latency.[50] Nevertheless, NF-κB is strongly and persistently activated in ATL cells through IKK,[9] although the mechanism of IKK activation has remained unknown. The findings in our present study demonstrate the aberrant expression of *NIK* at the pretranslational level in ATL cells derived from 15 of 21 patients. This overexpression does not seem to correlate with the patients' age, sex, disease type, or percentage of abnormal lymphocytes (Table S1). Further studies will be required to clarify potentially NIK-independent NF-κB activation in the other 6 cases. The stable expression of functional NIK in fibroblasts, but not that of its catalytically inactive mutant, causes cellular transformation and persistent NF-κB activation with molecular features quite similar to those reported previously in ATL cells. These include the rapid

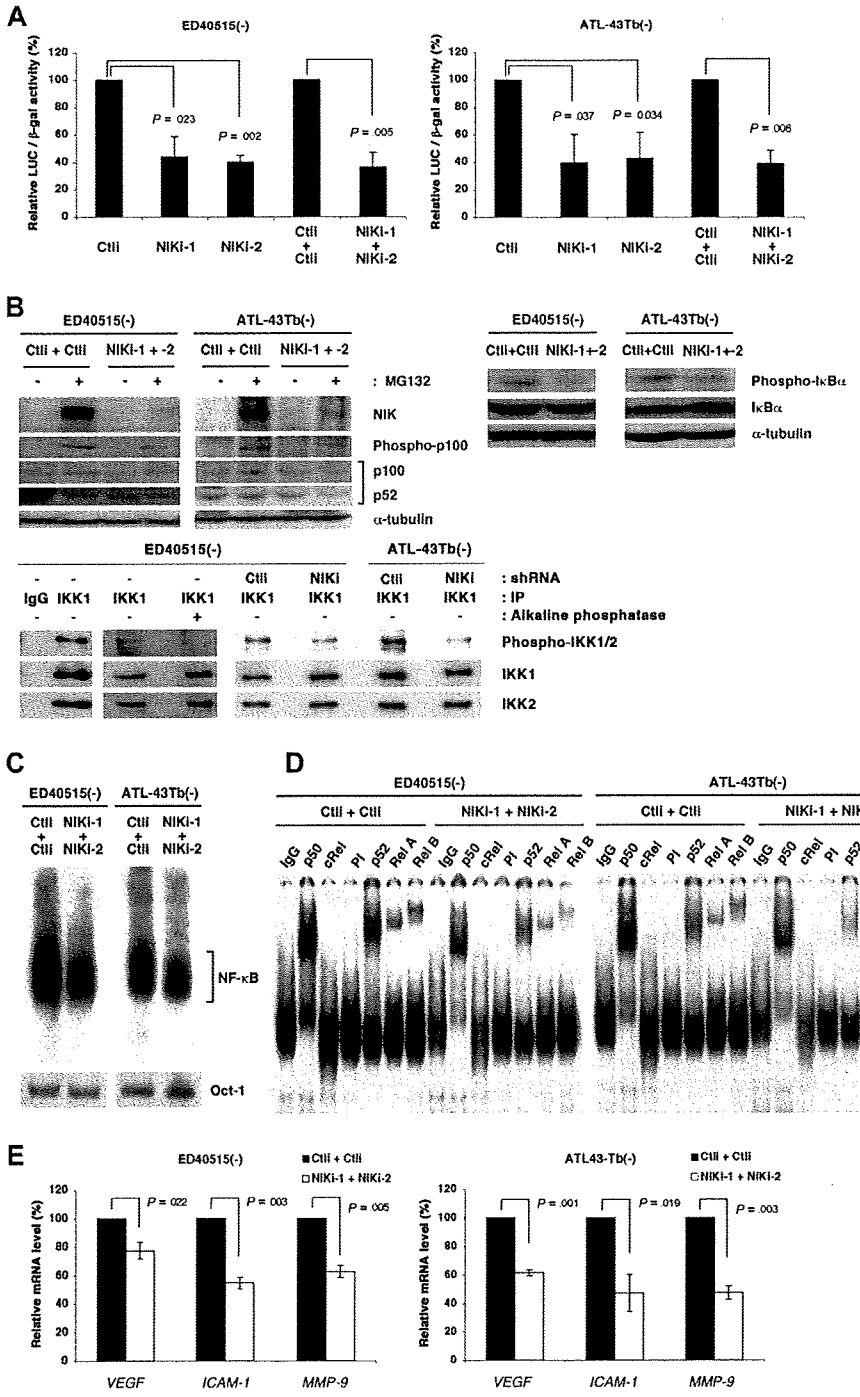


**Figure 6. Depletion of NIK suppresses NF-κB-dependent transcription in ATL cells.** (A) ED40515(−) and ATL-43Tb(−) cells were infected with lentiviral vectors expressing *Renilla luciferase* (Ctli) or *NIK*-specific shRNAs (NIKi-1 or NIKi-2). In parallel, ED40515(−) and ATL-43Tb(−) cells were infected with lentiviral vectors expressing Ctli or NIKi-1 shRNAs, and 24 hours later, these cells were super-infected with lentiviral vectors expressing Ctli or NIKi-2 shRNAs. Twenty-four hours after infection, cells were selected with puromycin for 2 days. Puromycin-resistant cells were then transfected with 2 μg of IgκCona-Luc and 2 μg EF1-LacZ. Luciferase (LUC) activity was determined 48 hours after transfection and normalized to β-gal activity. Relative luciferase activities, in comparison with control cells, 100 are shown. Data are expressed as mean plus or minus SD of 3 independent experiments. *P* values are versus control (Ctli). (B) Super-infected cells were treated with or without MG132 (20 μM) for 3 hours and subjected to SDS-PAGE and immunoblotting with anti-NIK (#4994), antiphosphorylated p100, or anti-α-tubulin antibodies. Whole-cell extracts (30 μg) from these cells were analyzed by SDS-PAGE and immunoblotting with antiphospho-IκBα, anti-IκBα, or anti-α-tubulin antibodies. Cytoplasmic extracts prepared from ED40515(−) cells infected or not with lentivirus were precleared and immunoprecipitation was performed, using anti-IKK1 monolconal antibody or its isotype IgG (IgG). After 3 washes with TNT buffer, immune complexes were treated or not with Shrimp Akaline Phosphatase (Takara Bio) and then subjected to SDS-PAGE and immunoblotting with antiphospho-IKK1/2, anti-IKK1, or anti-IKK2 antibodies. (C) A total of 5 μg of nuclear extracts prepared from lentivirus-infected cells shown in panel B were analyzed by EMSA, using oligonucleotides encoding the NF-κB–binding sequence or Oct-1–binding sequence as probes. (D) Nuclear extracts (5 μg) from lentivirus-infected cells shown in panel B were preincubated for 30 minutes with purified mouse IgG, anti-p50, anti-cRel antibody, preimmune (PI), anti-p50, anti-RelA or anti-RelB sera, and then subjected to EMSA with the NF-κB–specific probe. (E) Total RNAs from lentivirus-infected cells shown in panel B were examined by quantitative RT-PCR for *VEGF*, *ICAM-1*, and *MMP-9* mRNA levels. Each mRNA level was normalized to *18S* RNA. Relative mRNA levels, in comparison with control cells, 100 are shown. Data are expressed as mean plus or minus SD of 3 independent experiments. *P* values are versus control (Ctli + Ctli).

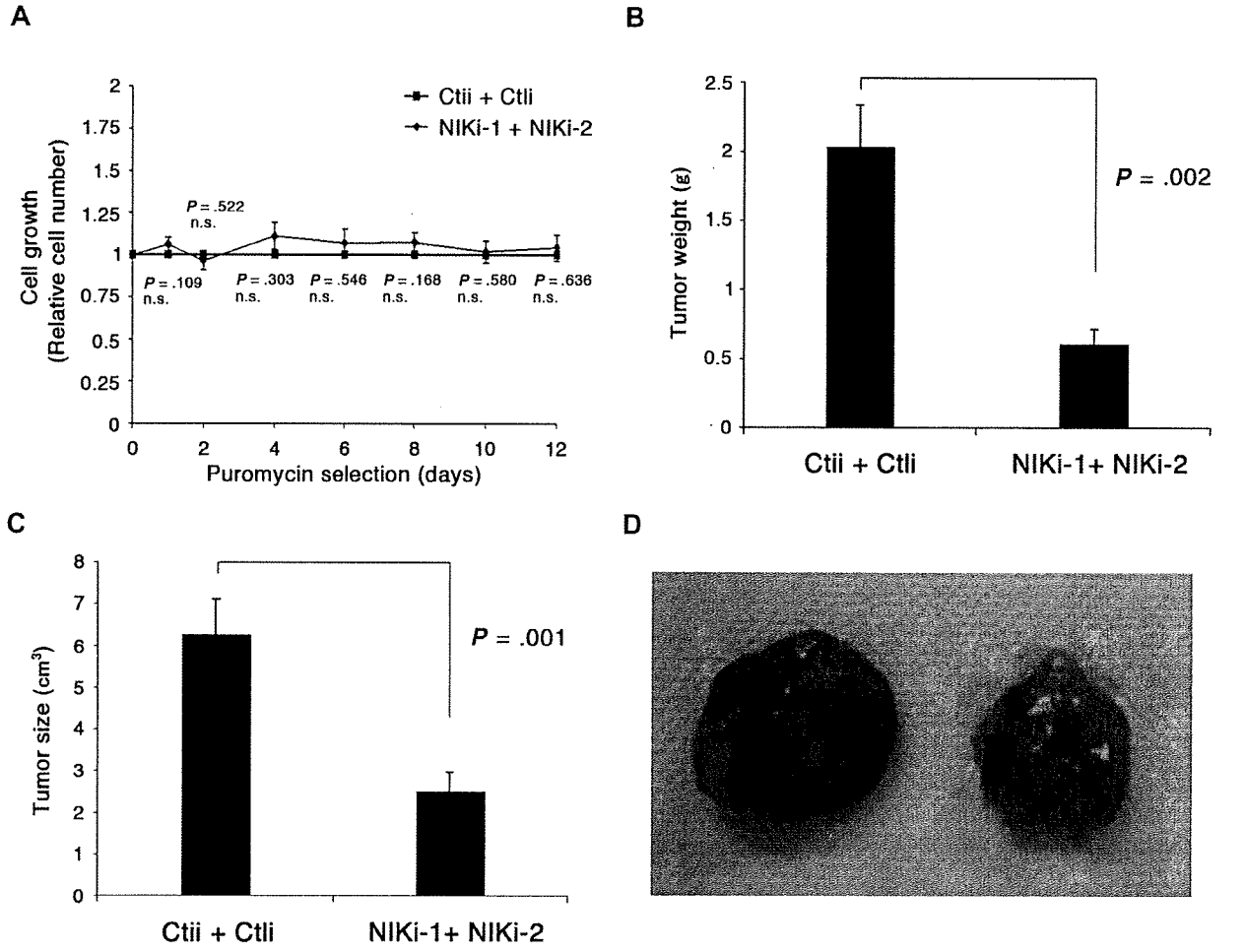


**Figure 7. Depletion of NIK in ATL cells suppresses tumor formation in NOD-SCID/γc$^{null}$ (NOG) mice.** (A) Pools of ED40515(−) cells expressing Ctli or NIKi-1 and -2, shown in Figure 6B, C, D, and E, were analyzed for cell growth in vitro by the trypan blue staining method. Relative cell numbers, in comparison with control cells (arbitrarily set at 1), are shown. Data are expressed as mean plus or minus SD of 3 independent experiments. *P* values are vs control (Ctli + Ctli). n.s. indicates no significant difference. (B-D) NOG mice were inoculated subcutaneously in the postauricular region with the puromycin-resistant ED-40515(−) cells (5 × 10$^6$). Tumor formation in mice was evaluated 2 weeks after inoculation. Tumor weight (B) and size (C) relative to those of tumors formed in mice inoculated with ED40515(−) cells expressing Ctli are shown. (D) Photographs of tumors formed 2 weeks after cell inoculation. Each result was obtained from 5 different mice (means are shown [error bars]). *P* values are versus control (Ctli + Ctli).

loss of IKK activity after protein synthesis inhibition and the superinduction of IKK activity in the presence of MG132.[11] Moreover, RNA interference studies have also indicated that the deregulated NIK expression is the principal cause of constitutive NF-κB activation in ATL cells. In line with a previous report by Ramakrishnan et al, which showed that the induction of IκBα degradation by CD70, CD40 ligand, and BLyS/BAFF is dependent on the function of NIK,[18] we find in our present experiments that the stable expression of NIK induces IκBα phosphorylation and the formation of DNA binding complexes containing not only p50 and RelB, but also RelA both in wild-type and in NEMO-deficient rat fibroblasts. This indicates that NIK can stimulate the canonical pathway characterized by IκBα phosphorylation and RelA activation and that NIK does not require NEMO for it. Interestingly, the forced expression of SR-IκBα in these fibroblasts abolishes the transformed phenotype and suppresses constitutive NF-κB activity, with the p100 and p52 expression levels being diminished simultaneously, probably because p100 expression is largely dependent on NF-κB activity.[51] RelB expression is also known to be controlled by NF-κB,[52] suggesting that the noncanonical pathway of NF-κB activation does not work independently but rather coincides with NF-κB activation through the canonical pathway under stable conditions.

H-RS cells were also found to overexpress NIK, including its transcripts, in this study. Earlier reports have described 2 potential mechanisms of constitutive NF-κB activation in H-RS cells: persistent signaling from receptors that cause NF-κB activation, such as CD30, CD40, and RANK as well as a CD40-like molecule latent membrane protein 1 of the Epstein-Barr virus; and disruption of IκBα-dependent suppression resulting from the mutation of this gene.[32,48] The H-RS cell lines used in this study are Epstein-Barr virus-negative, and neither HDLM-2 nor L540 cells harbor mutations in their *IκB* genes. Indeed, CD30, CD40, and RANK were all found to be expressed in the H-RS cell lines used in this study, but we envisage that the aberrant expression of NIK is a distinct mechanism underlying the persistent NF-κB activation in these cells. It is partly because these TNF family receptor molecules, when stimulated or overexpressed transiently in cultured cells, elevate the NIK protein expression levels with a concomitant reduction in TRAF3 but do not increase *NIK* mRNA.[19,20]

Whereas the transient stimulation of a B-cell line with BAFF or anti-CD40 antibody stabilizes the NIK protein at the posttranslational level and does not up-regulate its mRNA expression,[20] NIK was observed to be constitutively overexpressed in ATL and H-RS cells at the pretranslational level. These differing mechanisms of NIK regulation may not be all that surprising, however, in light of the transient vs persistent nature of the activation of NF-κB. The barely detectable levels of steady-state NIK protein expression and its robust accumulation after proteasome inhibition in ATL and H-RS cells further suggest that the proteasome-dependent degradation of NIK occurs rapidly in tumor cells as in normal cells, although we cannot rule out the possibility that TNF family receptors known to be overexpressed in H-RS cells influence the stability of NIK to some extent. This point is currently very difficult to address because the protein amount of NIK in the absence of the proteasome inhibitor is quite limited. At least 3 mechanisms of pretranslational induction of NIK are plausible: the stabilization of *NIK* transcripts, transcriptional activation and/or amplification of the *NIK* gene. It should be noted that the stability of *NIK* mRNA in ATL cells was similar to that in control cells, suggesting that NIK expression is deregulated in ATL cells at the level of mRNA production. In this regard, we are currently analyzing the regulatory region of the *NIK* gene in normal and cancer cells.

We detected NIK in whole-cell lysates only when the cells themselves were treated with the proteasome inhibitor, MG132. It is possible that the expression of the NIK protein is tightly regulated under detectable levels in resting normal cells. However, in ATL and H-RS cells, enhanced NIK production, although still not detectable by simple immunoblotting, may be sufficient to cause its deregulated activity toward IKK. During the manuscript preparation, 2 reports demonstrated deregulated expression of NIK because of mutations in *TRAF3, CYLD*, or *NIK* itself in multiple myeloma cells.[16,17] In case of ATL cells, formation of a fusion protein after genomic rearrangement seems to be unlikely based on the apparently normal size of the protein. At present, the mechanism of overproduction of *NIK* mRNA in ATL cells remains to be determined, but the fluorescence in situ hybridization results suggest that aberrant NIK expression in ATL cells is not the result of genomic abnormalities, such as amplification or translocation.

Successful anticancer drug or gene therapies can be conducted in a number of ways, including the general administration of particular reagents that mechanistically work exclusively on cancer cells, or delivering conventional anticancer reagents specifically to cancer cells. The former strategy is likely to be more promising in the case of hematopoietic cancers. In this regard, NIK could be an attractive molecular target for ATL and Hodgkin lymphoma therapy, although the physiologic functions of NIK in human adults remain unknown. Suppressing high NF-κB activity levels by targeting NIK may also sensitize these cancer cells to commonly used anticancer agents.

## Acknowledgments

The authors thank all of the ATL patients who donated blood samples for use in this study, Dr K. Yamaguchi and the Joint Study on Predisposing Factors of ATL Development for providing and analyzing sample blood, and the following researchers for donating invaluable reagents: Dr M. Maeda (Kyoto University, Kyoto, Japan) for the ED40515(−) and ATL-43Tb(−) cells, Dr D. Goeddel (Amgen, Thousand Oaks, CA) for *NIK* cDNAs, Dr N.R. Rice and Dr A. Israël (Institut Pasteur Paris, Paris, France) for p50, RelA, and RelB antisera, Dr T. Kitamura (University of Tokyo, Tokyo, Japan) for Plat-E cells, Dr I.S.Y. Chen (UCLA, Los Angeles, CA) for pHCMV-VSVG and pCMVΔR8.2 packaging plasmids, and Dr H. Miyoshi (RIKEN Tsukuba Institute, Tsukuba, Japan) for CS-CDF-CG-PRE plasmid. The authors also thank Dr G. Courtois (INSERM, Paris, France) and the members of the Department of Molecular Virology for helpful discussions.

This work was supported by research grants from the Ministry of Health and Labor Sciences (HIV/AIDS, H18-005) (Naoki Yamamoto) and from the Ministry of Education, Culture, Sports, Science and Technology of Japan (18390145; Naoki Yamamoto) and (17013029; S.Y.).

## Authorship

Contribution: Y.S., T.S., and S.Y. designed the study; Y.S., Norio Yamamoto, H.S., V.J.M.B., Y.I., K.M., X.Q., I.I., J.I., and S.Y. carried out the research; M.Z.D. carried out the animal experiments; A.U. and T.W. collected and analyzed sample blood from ATL patients; T.M. contributed to lentiviral vector constructions; Y.S. and S.Y. analyzed the data; T.S., Naoki Yamamoto and S.Y. controlled the data; Y.S. and S.Y. wrote the paper; all authors checked the final version of the manuscript.

Conflict-of-interest disclosure: The authors declare no competing financial interests.

Correspondence: Shoji Yamaoka, Department of Molecular Virology, Graduate School of Medicine, Tokyo Medical and Dental University, 1-5-45, Yushima, Bunkyo-ku, Tokyo, 113-8510, Japan; e-mail: shojmmb@tmd.ac.jp.

## References

1. Baldwin AS Jr. Series introduction: the transcription factor NF-kappaB and human disease. J Clin Invest. 2001;107:3-6.
2. Hayden MS, Ghosh S. Signaling to NF-kappaB. Genes Dev. 2004;18:2195-2224.
3. Xiao G, Rabson AB, Young W, Qing G, Qu Z. Alternative pathways of NF-kappaB activation: a double-edged sword in health and disease. Cytokine Growth Factor Rev. 2006;17:281-293.
4. Coope HJ, Atkinson PG, Huhse B, et al. CD40 regulates the processing of NF-kappaB2 p100 to p52. EMBO J. 2002;21:5375-5385.
5. Claudio E, Brown K, Park S, Wang H, Siebenlist U. BAFF-induced NEMO-independent processing of NF-kappa B2 in maturing B cells. Nat Immunol. 2002;3:958-965.
6. Karin M, Cao Y, Greten FR, Li ZW. NF-kappaB in cancer: from innocent bystander to major culprit. Nat Rev Cancer. 2002;2:301-310.
7. Jost PJ, Ruland J. Aberrant NF-{kappa}B signaling in lymphoma: mechanisms, consequences and therapeutic implications. Blood. 2006;109:2700-2707.
8. Ni H, Ergin M, Huang Q, et al. Analysis of expression of nuclear factor kappa B (NF-kappa B) in multiple myeloma: downregulation of NF-kappa B induces apoptosis. Br J Haematol. 2001;115:279-286.
9. Hironaka N, Mochida K, Mori N, Maeda M, Yamamoto N, Yamaoka S. Tax-independent constitutive IkappaB kinase activation in adult T-cell leukemia cells. Neoplasia. 2004;6:266-278.
10. Nonaka M, Horie R, Itoh K, Watanabe T, Yamamoto N, Yamaoka S. Aberrant NF-kappaB2/p52 expression in Hodgkin/Reed-Sternberg cells and CD30-transformed rat fibroblasts. Oncogene. 2005;24:3976-3986.
11. Miura H, Maeda M, Yamamoto N, Yamaoka S. Distinct IkappaB kinase regulation in adult T cell leukemia and HTLV-I-transformed cells. Exp Cell Res. 2005;308:29-40.
12. Dejardin E, Bonizzi G, Bellahcene A, Castronovo V, Merville MP, Bours V. Highly-expressed p100/p52 (NFKB2) sequesters other NF-kappa B-related proteins in the cytoplasm of human breast cancer cells. Oncogene. 1995;11:1835-1841.
13. Lessard L, Begin LR, Gleave ME, Mes-Masson AM, Saad F. Nuclear localization of nuclear factor-kappaB transcription factors in prostate cancer: an immunohistochemical study. Br J Cancer. 2005;93:1019-1023.
14. Chandler NM, Canete JJ, Callery MP. Increased

expression of NF-kappa B subunits in human pancreatic cancer cells. J Surg Res. 2004;118:9-14.

15. Bours V, Dejardin E, Goujon-Letawe F, Merville MP, Castronovo V. The NF-kappa B transcription factor and cancer: high expression of NF-kappa B- and I kappa B-related proteins in tumor cell lines. Biochem Pharmacol. 1994;47:145-149.
16. Annunziata CM, Davis RE, Demchenko Y, et al. Frequent engagement of the classical and alternative NF-kappaB pathways by diverse genetic abnormalities in multiple myeloma. Cancer Cell. 2007;12:115-130.
17. Keats JJ, Fonseca R, Chesi M, et al. Promiscuous mutations activate the noncanonical NF-kappaB pathway in multiple myeloma. Cancer Cell. 2007;12:131-144.
18. Ramakrishnan P, Wang W, Wallach D. Receptor-specific signaling for both the alternative and the canonical NF-kappaB activation pathways by NF-kappaB-inducing kinase. Immunity. 2004;21:477-489.
19. Liao G, Zhang M, Harhaj EW, Sun SC. Regulation of the NF-kappaB-inducing kinase by tumor necrosis factor receptor-associated factor 3-induced degradation. J Biol Chem. 2004;279:26243-26250.
20. Qing G, Qu Z, Xiao G. Stabilization of basally translated NF-kappaB-inducing kinase (NIK) protein functions as a molecular switch of processing of NF-kappaB2 p100. J Biol Chem. 2005;280:40578-40582.
21. Maeda M, Shimizu A, Ikuta K, et al. Origin of human T-lymphotrophic virus I-positive T cell lines in adult T cell leukemia: analysis of T cell receptor gene rearrangement. J Exp Med. 1985;162:2169-2174.
22. Yagi H, Nomura T, Nakamura K, et al. Crucial role of FOXP3 in the development and function of human CD25$^{+}$CD4$^{+}$ regulatory T cells. Int Immunol. 2004;16:1643-1656.
23. Sugamura K, Fujii M, Kannagi M, Sakitani M, Takeuchi M, Hinuma Y. Cell surface phenotypes and expression of viral antigens of various human cell lines carrying human T-cell leukemia virus. Int J Cancer. 1984;34:221-228.
24. Foley GE, Lazarus H, Farber S, Uzman BG, Boone BG, McCarthy RE. Continuous cultured human lymphoblasts from peripheral blood of a child with acute leukemia. Cancer. 1965;18:522-529.
25. Weiss A, Wiskocil RL, Stobo JD. The role of T3 surface molecules in the activation of human T cells: a two-stimulus requirement for IL 2 production reflects events occurring at pre-translational level. J Immunol. 1984;133:123-128.
26. Yamaoka S, Courtois G, Bessia C, et al. Complementation cloning of NEMO, a component of the IkappaB kinase complex essential for NF-kappaB activation. Cell. 1998;93:1231-1240.
27. Chinanonwait N, Miura H, Yamamoto N, Yamaoka S. A recessive mutant cell line with a constitutive IkappaB kinase activity. FEBS Lett. 2002;531:553-560.
28. Morita S, Kojima T, Kitamura T. Plat-E: an efficient and stable system for transient packaging of retroviruses. Gene Ther. 2000;7:1063-1066.
29. Yamaoka S, Inoue H, Sakurai M, et al. Constitutive activation of NF-kappa B is essential for transformation of rat fibroblasts by the human T-cell leukemia virus type I Tax protein. EMBO J. 1996;15:873-887.
30. Munoz E, Courtois G, Veschambre P, Jalinot P, Israël A. Tax induces nuclear translocation of NF-kappa B through dissociation of cytoplasmic complexes containing p105 or p100 but does not induce degradation of I kappa B alpha/MAD3. J Virol. 1994;68:8035-8044.
31. Dewan MZ, Terashima K, Taruishi M, et al. Rapid tumor formation of human T-cell leukemia virus type 1-infected cell lines in novel NOD-SCID/$\gamma c^{null}$ mice: suppression by an inhibitor against NF-κB. J Virol. 2003;77:5286-5294.
32. Krappmann D, Emmerich F, Kordes U, Scharschmidt E, Dorken B, Scheidereit C. Molecular mechanisms of constitutive NF-kappaB/Rel activation in Hodgkin/Reed-Stemberg cells. Oncogene. 1999;18:943-953.
33. Wood KM, Roff M, Hay RT. Defective IkappaBalpha in Hodgkin cell lines with constitutively active NF-kappaB. Oncogene. 1998;16:2131-2139.
34. Mori N, Fujii M, Ikeda S, et al. Constitutive activation of NF-kappaB in primary adult T-cell leukemia cells. Blood. 1999;93:2360-2368.
35. Yemelyanov A, Gasparian A, Lindholm P, et al. Effects of IKK inhibitor PS1145 on NF-kappaB function, proliferation, apoptosis and invasion activity in prostate carcinoma cells. Oncogene. 2006;25:387-398.
36. Farina AR, Tacconelli A, Vacca A, Maroder M, Gulino A, Mackay AR. Transcriptional up-regulation of matrix metalloproteinase-9 expression during spontaneous epithelial to neuroblast phenotype conversion by SK-N-SH neuroblastoma cells, involved in enhanced invasivity, depends upon GT-box and nuclear factor kappaB elements. Cell Growth Differ. 1999;10:353-367.
37. Collins T, Read MA, Neish AS, Whitley MZ, Thanos D, Maniatis T. Transcriptional regulation of endothelial cell adhesion molecules: NF-kappa B and cytokine-inducible enhancers. FASEB J. 1995;9:899-909.
38. El-Sabban ME, Merhi RA, Haidar HA, et al. Human T-cell lymphotropic virus type 1-transformed cells induce angiogenesis and establish functional gap junctions with endothelial cells. Blood. 2002;99:3383-3389.
39. Mori N, Sato H, Hayashibara T, et al. Human T-cell leukemia virus type I Tax transactivates the matrix metalloproteinase-9 gene: potential role in mediating adult T-cell leukemia invasiveness. Blood. 2002;99:1341-1349.
40. Hayashibara T, Yamada Y, Onimaru Y, et al. Matrix metalloproteinase-9 and vascular endothelial growth factor: a possible link in adult T-cell leukaemia cell invasion. Br J Haematol. 2002;116:94-102.
41. Fukudome K, Furuse M, Fukuhara N, Orita T, Hinuma Y. Strong induction of ICAM-1 in human T cells transformed by human T-cell leukemia virus type 1 and depression of ICAM-1 or LFA-1 in adult T-cell leukemia-derived cell lines. Int J Cancer. 1992;52:418-427.
42. Mori N, Yamada Y, Ikeda S, et al. Bay 11–7082 inhibits transcription factor NF-kappaB and induces apoptosis of HTLV-I-infected T-cell lines and primary adult T-cell leukemia cells. Blood. 2002;100:1828-1834.
43. Bargou RC, Emmerich F, Krappmann D, et al. Constitutive nuclear factor-kappaB-RelA activation is required for proliferation and survival of Hodgkin's disease tumor cells. J Clin Invest. 1997;100:2961-2969.
44. Yang J, Amiri KI, Burke JR, Schmid JA, Richmond A. BMS-345541 targets inhibitor of kappaB kinase and induces apoptosis in melanoma: involvement of nuclear factor kappaB and mitochondria pathways. Clin Cancer Res. 2006;12:950-960.
45. Gasparian AV, Yao YJ, Kowalczyk D, et al. The role of IKK in constitutive activation of NF-kappaB transcription factor in prostate carcinoma cells. J Cell Sci. 2002;115:141-151.
46. Wang CY, Cusack JC Jr, Liu R, Baldwin AS Jr. Control of inducible chemoresistance: enhanced anti-tumor therapy through increased apoptosis by inhibition of NF-kappaB. Nat Med. 1999;5:412-417.
47. Gilmore TD, Herscovitch M. Inhibitors of NF-kappaB signaling: 785 and counting. Oncogene. 2006;25:6887-6899.
48. Braun T, Carvalho G, Fabre C, Grosjean J, Fenaux P, Kroemer G. Targeting NF-kappaB in hematologic malignancies. Cell Death Differ. 2006;13:748-758.
49. Courtois G, Gilmore TD. Mutations in the NF-kappaB signaling pathway: implications for human disease. Oncogene. 2006;25:6831-6843.
50. Sun SC, Yamaoka S. Activation of NF-kappaB by HTLV-I and implications for cell transformation. Oncogene. 2005;24:5952-5964.
51. Liptay S, Schmid RM, Nabel EG, Nabel GJ. Transcriptional regulation of NF-kappa B2: evidence for kappa B-mediated positive and negative autoregulation. Mol Cell Biol. 1994;14:7695-7703.
52. Bren GD, Solan NJ, Miyoshi H, Pennington KN, Pobst LJ, Paya CV. Transcription of the RelB gene is regulated by NF-kappaB. Oncogene. 2001;20:7722-7733.

# SOCS1 is an inducible host factor during HIV-1 infection and regulates the intracellular trafficking and stability of HIV-1 Gag

Akihide Ryo[a,b,c], Naomi Tsurutani[d], Kenji Ohba[b,e], Ryuichiro Kimura[e,f], Jun Komano[b], Mayuko Nishi[a], Hiromi Soeda[a], Shinichiro Hattori[b], Kilian Perrem[g], Mikio Yamamoto[h], Joe Chiba[f], Jun-ichi Mimaya[i], Kazuhisa Yoshimura[j], Shuzo Matsushita[j], Mitsuo Honda[b], Akihiko Yoshimura[k], Tatsuya Sawasaki[l], Ichiro Aoki[a], Yuko Morikawa[d], and Naoki Yamamoto[b,c]

[a]Department of Pathology, Yokohama City University School of Medicine, 3-9 Fuku-ura, Kanazawa-ku, Yokohama 236-0004, Japan; [b]AIDS Research Center, National Institute of Infectious Diseases, 1-23-1 Toyama, Shinjuku-ku, Tokyo 162-8640, Japan; [d]Kitasato Institute for Life Sciences, Kitasato University, Shirokane 5-9-1, Minato-ku, Tokyo 108-8641, Japan; [e]Department of Molecular Virology, Graduate School of Medicine, Tokyo Medical and Dental University, 1-5-45 Yushima, Bunkyo-ku, Tokyo 113-8519, Japan; [f]Molecular Oncology Laboratory, Department of Pathology, Royal College of Surgeons in Ireland, Smurfit Building, Beaumont Hospital, Dublin 9, Ireland; [h]Department of Biochemistry II, National Defense Medical College, 3-2 Namiki, Tokorozawa-shi, Saitama 359-8513, Japan; [g]Department of Biological Science and Technology, Science University of Tokyo, 2641 Yamazaki, Noda, Chiba 278-8510, Japan; [i]Division of Hematology and Oncology, Shizuoka Children's Hospital, 860 Urushiyama, Aoi-ku, Shizuoka 420-8660, Japan; [j]Division of Clinical Retrovirology and Infectious Diseases, Center for AIDS Research, Graduate School of Medical Sciences, Kumamoto University, Kumamoto 860-0811, Japan; [k]Division of Molecular and Cellular Immunology, Medical Institute of Bioregulation, Kyushu University, Fukuoka 812-8582, Japan; and [l]Cell Free Science and Research Center, Ehime University, Ehime 790-8577, Japan

Edited by Robert C. Gallo, University of Maryland, Baltimore, MD, and approved November 19, 2007 (received for review May 24, 2007)

**Human immunodeficiency virus type 1 (HIV-1) utilizes the macromolecular machinery of the infected host cell to produce progeny virus. The discovery of cellular factors that participate in HIV-1 replication pathways has provided further insight into the molecular basis of virus–host cell interactions. Here, we report that the suppressor of cytokine signaling 1 (SOCS1) is an inducible host factor during HIV-1 infection and regulates the late stages of the HIV-1 replication pathway. SOCS1 can directly bind to the matrix and nucleocapsid regions of the HIV-1 p55 Gag polyprotein and enhance its stability and trafficking, resulting in the efficient production of HIV-1 particles via an IFN signaling-independent mechanism. The depletion of SOCS1 by siRNA reduces both the targeted trafficking and assembly of HIV-1 Gag, resulting in its accumulation as perinuclear solid aggregates that are eventually subjected to lysosomal degradation. These results together indicate that SOCS1 is a crucial host factor that regulates the intracellular dynamism of HIV-1 Gag and could therefore be a potential new therapeutic target for AIDS and its related disorders.**

AIDS | pathogenesis | drug target | lysozyme

Human immunodeficiency virus type 1 (HIV-1) infection is a multistep and multifactorial process mediated by a complex series of virus–host cell interactions (1, 2). The molecular interactions between host cell factors and HIV-1 are vital to our understanding of not only the nature of the resulting viral replication, but also the subsequent cytopathogenesis that occurs in the infected cells (3). The characterization of the genes in the host cells that are up- or down-regulated upon HIV-1 infection could therefore provide a further elucidation of virus–host cell interactions and identify putative molecular targets for the HIV-1 replication pathway (4).

The HIV-1 p55 Gag protein consists of four domains that are cleaved by the viral protease concomitantly with virus release. This action generates the mature Gag protein comprising the matrix (MA/p17), capsid (CA/p24), nucleocapsid (NC/p7), and p6 domains, in addition to two small spacer peptides, SP1 and SP2 (5, 6). The N-terminal portion of MA, which is myristoylated, facilitates the targeting of Gag to the plasma membrane (PM), whereas CA and NC promote Gag multimerization. p6 plays a central role in the release of HIV-1 particles from PM by interacting with the vacuolar sorting protein Tsg101 and AIP1/ALIX (7–9). Several recent studies have implicated the presence of host factors in the control of the intracellular trafficking of Gag. AP-3δ is a recently characterized endosomal adaptor protein that binds directly to the MA region of Gag and enhances its targeting to the multivesicular body (MVB) during the early stages of particle assembly (10). The *trans*-Golgi network (TGN)-associated protein hPOSH plays another role in Gag transport by facilitating the egress of Gag cargo vesicles from the TGN, where it assembles with envelope protein (Env) before transport to PM (11). Although the involvement of these host proteins in the regulation of intracellular Gag trafficking has been proposed, the detailed molecular mechanisms underlying this process are still not yet well characterized.

In our current work, we demonstrate that the suppressor of cytokine signaling 1 (SOCS1) directly binds HIV-1 Gag and facilitates the intracellular trafficking and stability of this protein, resulting in the efficient production of HIV-1 particles. These results indicate that SOCS1 is a crucial host factor for efficient HIV-1 production and could be an intriguing molecular target for future treatment of AIDS and related diseases.

## Results

**SOCS1 Is Induced upon HIV-1 Infection and Facilitates HIV-1 Replication via Posttranscriptional Mechanisms.** We and others have shown that HIV-1 infection can alter cellular gene expression patterns, resulting in the modification of viral replication and impaired homeostasis in the host cells (4, 12). Hence, to elucidate further the genes and cellular pathways that participate in HIV-1 replication processes, we performed serial analysis of gene expression (SAGE) using either a HIV-1 or mock-infected human T cell line, MOLT-4 (12). Further detailed analysis of relatively low-abundance SAGE tags identified *SOCS1* as a preferentially up-regulated gene after HIV-1 infection. This finding was validated by both semiquantitative RT-PCR and immunoblotting analysis with anti-SOCS1 anti-

Author contributions: A.R. and N.T. contributed equally to this work; A.R., A.Y., Y.M., and N.Y. designed research; A.R., N.T., K.O., R.K., M.N., H.S., S.H., T.S., I.A., and Y.M. performed research; J.K., S.H., M.Y., J.C., J.-i.M., K.Y., S.M., M.H., and A.Y. contributed new reagents/analytic tools; A.R., N.T., K.O., M.N., H.S., K.P., M.Y., K.Y., S.M., T.S., I.A., Y.M., and N.Y. analyzed data; and A.R., K.P., and N.Y. wrote the paper.

The authors declare no conflict of interest.

This article is a PNAS Direct Submission.

Freely available online through the PNAS open access option.

[c]To whom correspondence may be addressed. E-mail: aryo@nih.go.jp or nyama@nih.go.jp.

This article contains supporting information online at www.pnas.org/cgi/content/full/0704831105/DC1.





www.pnas.org/cgi/doi/10.1073/pnas.0704831105